THERMALLY ACTUATED FLEXURE

A report submitted in fulfilment of the
design and build assignment in Precision Machine Design
by

Michael Erickson (800769005)

Chunjie Fan (800904460)

Gokul Mohandas (800964904)

Ameya Parab (800960115)

Under the guidance of

Dr. Stuart Smith

The University of North Carolina at Charlotte

The William States Lee College of Engineering

The Department of Mechanical Engineering

Abstract

Flexures are structures used for micrometer scale positioning with minimal frictional losses. In this project, the objective was to modify an existing thermally actuated, single degree of freedom flexure and to evaluate its operation and precision under an applied load in-line with the actuator and opposite the direction of travel. Several changes were made to improve the heating and cooling systems, which along with tuning of control systems reduction in noise and faster response times. Also for achieving the goal of 1000 N load capacity, the overall design of the flexure was changed, which includes an additional reinforcing outer steel frame, discarding the split clamp in original design and replacing it with a spring guided on a rod on the actuation side. Addition of threaded knob and compression plate assembly to apply tension to the spring. The fundamental working principle of the flexure was unchanged. It operates through the controlled expansion of a steel tube. The temperature and thermal expansion of the actuator was controlled using Ni-Cr wire coiled around the tube and cooling water flowing through the tube. The controlled thermal expansion of the tube generates the force that was converted into linear motion of the flexure stage. The tube actuator is thermally isolated on both ends using cooling water. A feedback loop was implemented using an IR based optical knife-edge sensor RPI 0352E to measure the linear displacement of the flexure stage. A PID controller implemented using LabVIEW and a myRIO was used to control the power supplied to the heating coil (Ni-Cr wire) and the cooling water pumps through individual power amplifiers. The new model was manufactured and tested. It was found that the flexure was successfully able to displace the projected 1000 N over a range of 100μm in 60 seconds. The flexure was able to retain a constant position with ±0.33μm variation. All the while, the cooling system effectively retained the frame and the flexure stage at 0.5°C above room temperature.

Table of Contents

List of Figures

List of Tables

1. Introduction

Flexures are frictionless devices which use the bending of load members to give micrometer (or in some cases nanometer) level precision. The flexures, contingent on their proper design, are very stiff and robust, lightweight and maintenance free. The arrangement of beams can be designed to be compliant in desired degree(s) of freedom (DOF), but relatively stiff in desired degree(s) of constraint (DOC). This allows engineers to provide motion only in desired directions, and constraint in other directions. However, due to the risk of bending failure of the flexure, the load capacity and range of motion is limited. In addition, it shows appreciable vibration and shock resistance. Due to these qualities, the flexure finds applications in fields of precision motion such as development of flexural couplings, mirror mounts, Scanning-tunneling microscope's (STM), mesoscale biomedical devices and fabrication of microelectronic components [1].

There are different types of flexure structures, monolithic, compound, crossed rotary, and disk or diaphragm flexure. Since single flexure, features are restricted in both travel capability and degrees of freedom available, compound flexure systems were designed using combinations of these component features. Using compound flexures, complex motion profiles with specific degrees of freedom and relatively long travel distances are possible. The flexure system has bending structures and spring elements. Most compound flexure designs are composed of three fundamental types of flexures. These include, pin flexure which is a thin bar or cylinder of material, with constrains 3 degree of freedom when geometry matches a notch cutout; Blade flexure which is thin sheet of material, which constrains 4 degrees of freedom; notch hinges comprise of a web between two notches, which constrains 5 degrees of freedom. Various notches are available namely in circular, elliptical and rectangular structure. There is a plethora of techniques for producing desired actuation in the flexure, namely voice coils, electromagnets, linear motors, rotary motors, Microelectromechanical systems (MEMS), piezoelectric, thermal, hydraulic etc. [1].

1.1. Introduction to thermal actuators

Thermal actuators have a heating mechanism, which supplies heat to an expansion member(s). The heat required for activation can be generated by several methods; the most utilized being the use of resistive one. This heat energy provides the driving force for expansion of this member, which can be transformed in rotation or translation continuous movement by activation of mechanisms. Thermal actuators either use expansion of a single member for axial/radial actuation or multiple members to produce a differential expansion and actuation in multiple directions depending upon the shape and design of actuator [2][3].

Thermal actuators are simple & rugged in construction and are relatively inexpensive to other actuation methods. In addition, they exhibit larger displacements and forces than other actuators and their thermal expansion is linearly related to the applied heat hence resulting in precise control. Heat is generated in accordance with the Lenz- Joule law by applying an electric current that flows through the device. The downside however being the high-power consumption of the actuator to produce appreciable displacements and a low energy efficiency with heat dissipation to the surrounding environment. Another main disadvantage is of thermal fatigue failure of expansion member and non-linear effects such as hysteresis phenomena. The repeated heating and cooling cycle of the actuator increases the risk of failure due to thermal fatigue. In addition, they show slower response time in comparison [2][3]. This disadvantage is less prominent in miniaturization conditions, which is the case in this project.

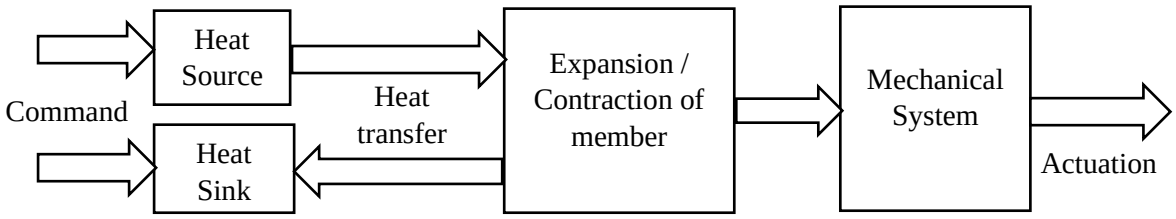

Figure 1.1: Thermal Actuator Schematic

1.2. Objective of project

Our primary objective in this project is to study the original design, test its limits, and then evaluate load capacity, repeatability, and range of motion for 1000N load capacity for 100um range. Secondary goals are to reduce system response time and reduce system noise. The global goal is to improve the performance of the existing flexure and evaluate its capabilities.

1.3. Scope of the project

The project focuses on the study of the original design of a thermally actuated flexure and develop and implement possible design improvements. The original model was re-assembled and tested/evaluated. The flexure's ability to traverse 100 um and its response time was tested. The CAD model of the original model was tested for stresses and failures in SOLIDWORKS software by application of 1000 N load to the base structure and based on this analysis, modifications to safely increase load capacity to 1000 N and faster performance were decided. These modifications were first implemented on the CAD model of the flexure and analyzed. Upon satisfaction, the final dimensions of the outside frame were decided.

2. Original Design

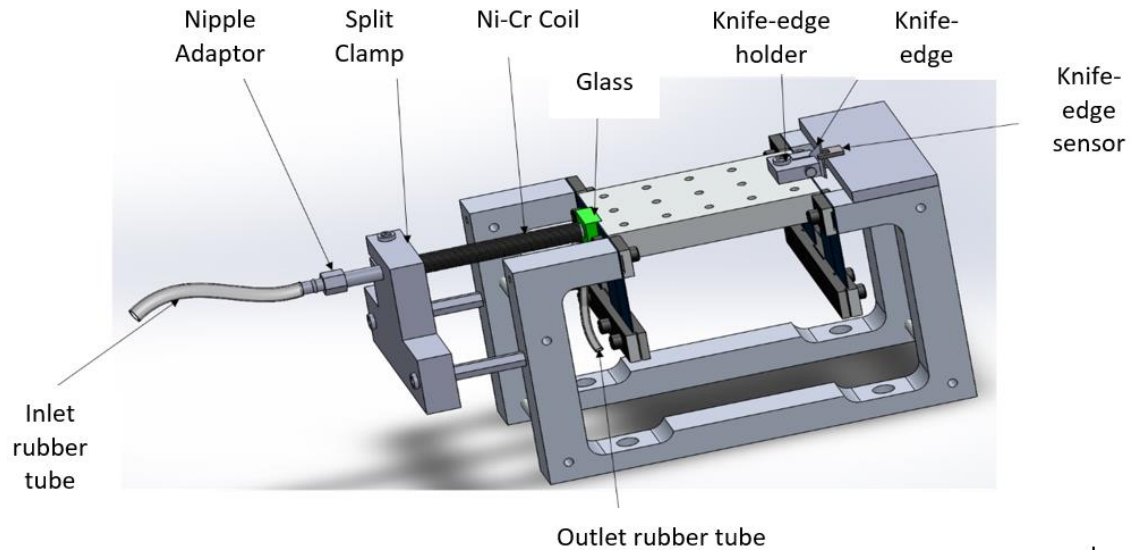

Figure 2.1: Original design of the thermally actuated flexure

The flexure system used in this project is a monolithic structure made of Aluminum. Leaf hinges are implemented which provides spring action. Leaf hinges has a thin sharp blade like design. The bending structures are notch hinges. Notch hinges of circular type were used in the original design. The overall design of the flexure of the system can be divided into 3 basic sections i.e. Flexure support structure, Heating & Cooling System and Control System [1].

2.1. Heating System

The heating system consists of Ni-Cr wire of 0.16 cm diameter wound around an Aluminum tube in a stacked manner using a lathe. The aluminum tube of length 15cm was used to get the required displacement of the flexure. The inner diameter and outer diameter of the aluminum tube is 0.305'' and 3/8'' respectively. It was threaded on one side for attaching a nipple adaptor for the rubber tubing, which was used for passing cooling water through the tube. A split clamp was used to hold the aluminum at one end and to restrict the expansion of aluminum to just one side. The other side of the aluminum tube, is connected to the flexure block through a multi layered sandwiched glass insulator with air in between the layers for better insulation.

2.2. Cooling System

The cooling system consists of a cooling water supply, which was pumped by a DC motor. This cooling water was pumped through high temperature resistant rubber inlet and outlet pipes to the hollow Aluminum tube to control its temperature. The flow of the water was controlled by the voltage input to the motor, which was in turn controlled by the motor driver in the Control system block.

The flexure structure consists of a base support, which holds the assembly together and has circular notches at the corners. It was made from two milled aluminum plates separated by standoffs, which were fastened at the ends. The flexure block, which was the element that actually translates the desired linear motion, is also made of solid aluminum block milled to size. Several holes in uniform fashion are bored into the block for weight reduction. It also allows attaching the required mechanism on top of the block. The return force to this block was provided by the leaf springs attached to the block and the base

structure on both ends. These leaves are thin leaves of blue spring steel, which were clamped to the base structure by flexure clamps made of anodized aluminum stock.

2.3. Control System

The control system block consists of linear displacement measurement and feedback mechanisms. The linear displacement of the flexure block was measured by means of an optical knife-edge sensor. The sensor was mounted on to the base structure. The knife-edge was mounted on the flexure block by means of a knife-edge holder made of 6061 aluminum, which holds the blade in the passage between the block, which was tightened by a screw. The sensor has a response of change in voltage with respect to the change in intensity of light passing though the sensor. This intensity of light was controlled by the penetration of knife-edge due to translation of moving block into the sensor area giving us voltage change and hence proportional displacement. The output voltage of the optical sensor was given to the Arduino Uno, which has an ADC card, which converts the analog signal from the knife-edge sensor into an arbitrary bit value that was calibrated and converted into a displacement. The pump and heating element were wired to the Arduino Uno through a motor driver. The motor driver regulates the power given to either the pump or the heating coil through pulse width modulation. The 10-amp power supply was connected to the power inlet on the motor driver and output channel one was connected to the pump and output channel two was connected to the heating element

3. Performance evaluation and modifications

Several tests were conducted to validate the claims of the original model for 100 um range and said response time of 40 seconds for covering this range [1]. Firstly, the model was assembled and the actual working state of each component was verified.

3.1. Thermal Evaluation

The heating system of the flexure was run independently to find out the maximum temperature that could be reached by the original aluminum rod actuator, the time required and the expansion of rod due to this heating. It was found that the Ni-Cr wire temperature reached 140 deg C and could remain constant. The aluminum tube's temperature was also found to be 140 deg C with some fractional difference as compared temperature of the Ni-Cr wire. This proves that sufficient heat from the Ni-Cr wire was transferred to the aluminum tube.

3.2. Optical Sensor Evaluation

The next step involved the validating the behavior of the optical system. The maximum range of the optical sensor mounted on a micrometer gauge for test purposes was found out to be 1mm (1000 um). In this range, the sensor showed linear behavior between 0.38 mm and 0.58 mm. Hence this range (200 um) of the optical sensor was taken as the working range of the sensor. The voltage response of the sensor with change in displacement is shown below:

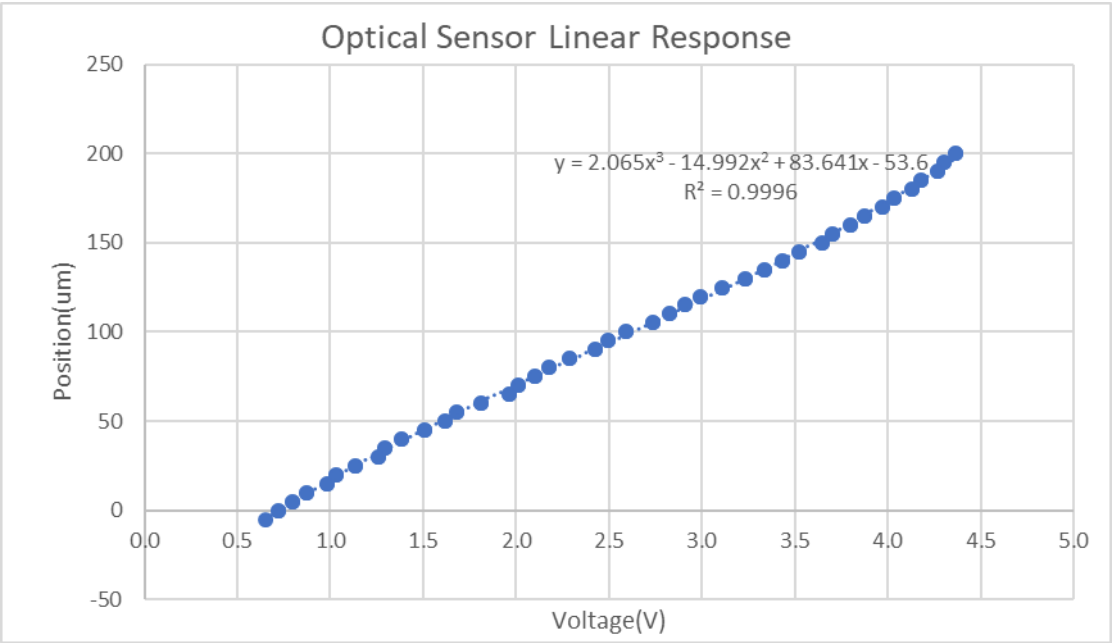

Figure 3.1: Voltage v/s Position response of IR optical sensor for linear range

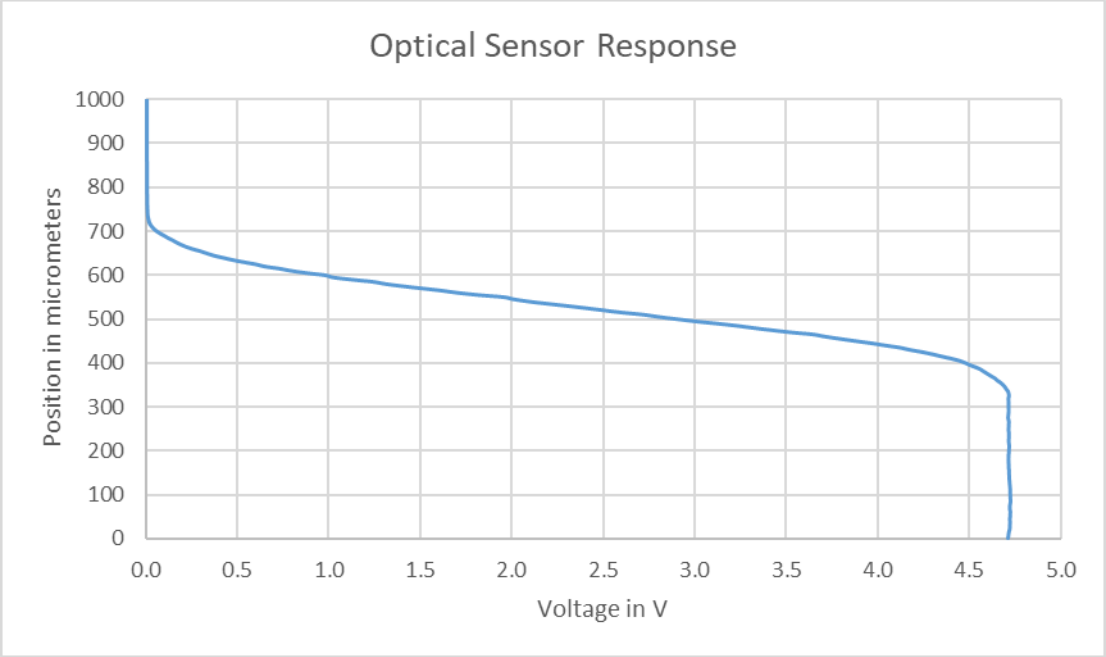

Figure 3.2: Voltage v/s Position response of IR optical sensor for complete range

3.3. CAD Model Simulation

The CAD model of the original design was analyzed for the new desired goal of 1000 N load capacity. The analysis was done using SOLIDWORKS. The results of the analysis are shown below:

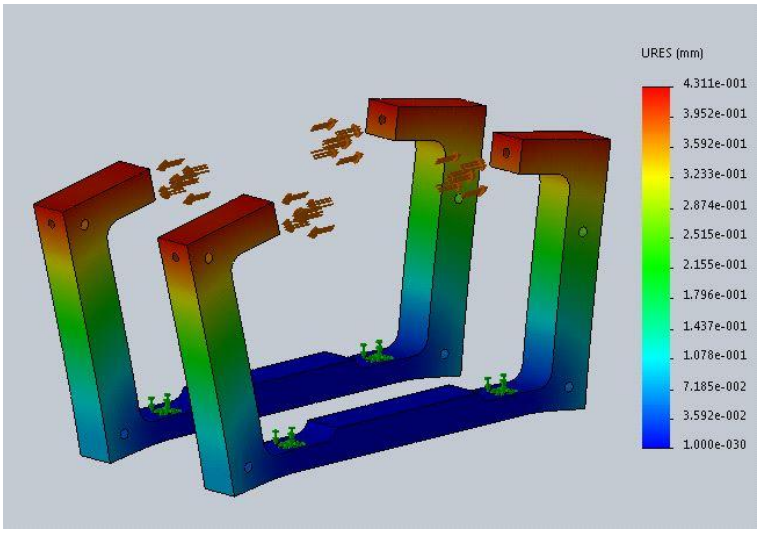

Figure 3.3: FEA Deflection Analysis of Original Base structure

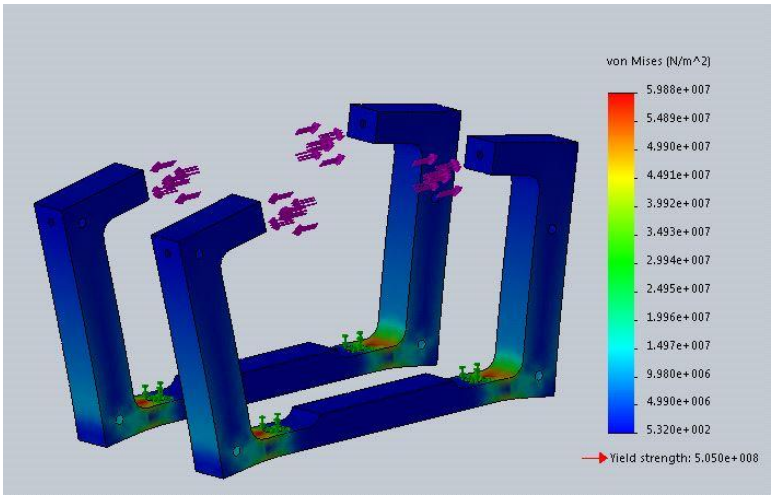

Figure 3.4: FEA Stress Analysis of Original Base structure

The maximum displacement was found to be 0.4 mm on both sides, i.e. 0.8 mm, which is significant in comparison to the original range of the flexure of 100 µm. Hence, the original frame clearly cannot support the proposed load of 1000 N load.

It was also found that on overloading the original design of the flexure, there was risk of the aluminum expansion rod expanding in the opposite direction as the spit clamp is unable to resist this expansion. Hence, the split clamp was discarded and the reinforced frame was used instead to provide normal force in the opposite direction. After brainstorming, several methods came into light, which could have been used. However, after careful trials, a monolithic outer frame design was finally decided. The design is shown as below:

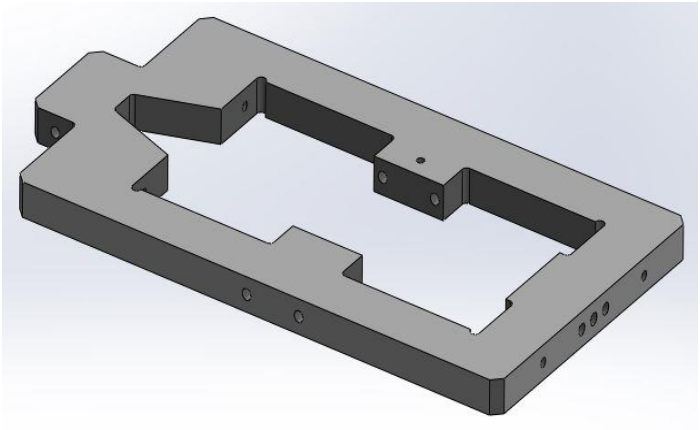

Figure 3.5: CAD Model of Outer Frame

The material of the frame was to be decided between steel and aluminum. Therefore, for both materials the frame were tested in SOLIDWORKS under 1000 N load assuming that the base structure is rigid body. The analysis of steel & aluminum frames is shown below:

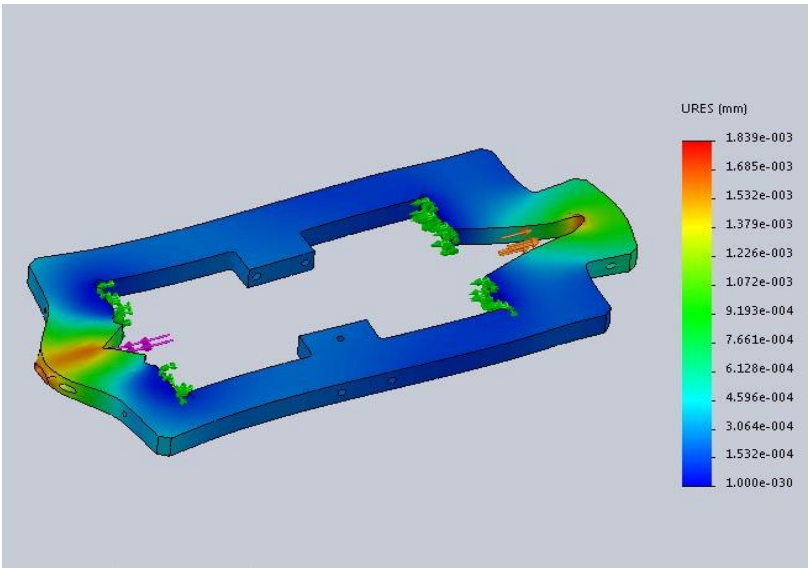

Figure 3.6: FEA Deflection Analysis of Aluminum frame

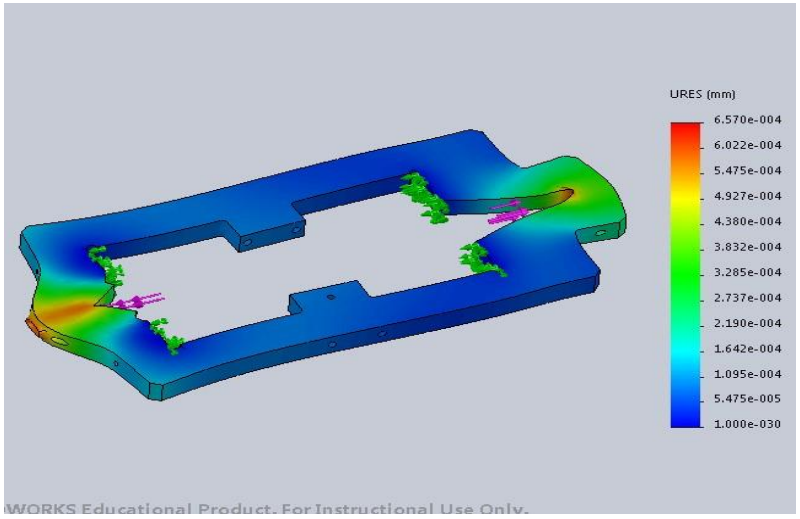

Figure 3.7: FEA Deflection Analysis of Steel frame

As the steel frame with very low deflection of 0.6 µm, showed result that is more promising. Hence, it was selected as a frame material with the only downside being the increase in the weight of the block.

Above, we have considered deflection of just the frame along the direction of actuation. However, deflection of the base structure (two 'C' shaped frames) were taken into consideration as it contributes significantly towards the overall deflection of the system. For that, assembly of the base structure and the reinforcing frame was analysed together.

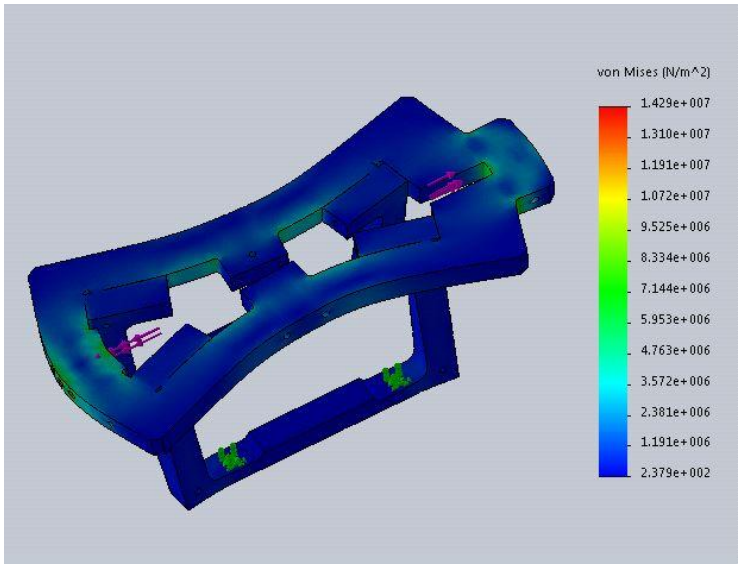

Figure 3.8: FEA Stress Analysis of Steel New Frame

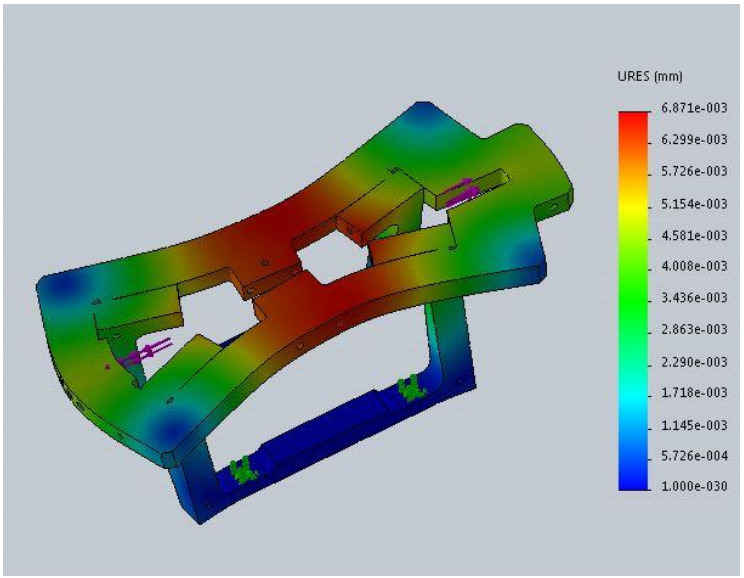

Figure 3.9: FEA Deflection Analysis of Steel New Frame

Total deflection was found to be 4µm on either side i.e. total 8µm. This deflection was very small compared to maximum range of 100 µm. On consulting with Dr. Smith, it was concluded that the results were within acceptable limits.

3.4. Modifications to original design

Due change in original design, the actuator was replaced to fit in the new outer frame. The actuator material was changed from aluminum to steel and Ni-Cr wire was coiled around it.

In addition, a compression spring was introduced on the actuation (output) side of the flexure connecting the flexure block and reinforcing frame. The stiffness of the spring was selected as 294.81 lbs. /in. (51.62 N/mm). The required loading of the spring was 225 lb (1000 N), requiring a compression distance of 0.76 in. The spring was selected based on its load capacity, extended length and outer diameter constraints. With the introduction of the spring, the stiffness of the flexure increased as compared to the stiffness of the assembly with just the frame, which was found insufficient in the original design. Increasing the stiffness of the spring expedited the load capacity of the flexure. Also, the stiffness of the spring was much lower than the stiffness of the rod (actuator) hence having less effect on its expansion.

The spring was guided using a rod attached to the frame so that the spring action is normal to both the frame and the moving block. The spring was compressed using a threaded knob, which is present at the outer end of the frame. This knob is in contact with a plate, which transfers the linear motion of the knob from the outer end, to the spring inside the frame by two guide pins. This block has two 'blind' holes (cavity) to accommodate the guide pins. On the opposite end, i.e. on the inner side of the frame is a dimensionally similar plate with identical holes for transferring the guide pins' motion to the spring except. On the inner-frame plate we have a 'through' central hole so that the guiding rod for the spring can pass through the plate. The knob moves inside or outside the frame per direction of rotation. This linear motion of the knob pushes the guide plates, compressing the spring. Hence, by tightening the knob we can change the pre-load acting on the spring, thereby accommodating variable loads. In addition, a vertical tapered hole was bored through both the guide pins and plates and pins were inserted to strengthen the interface between the guide pins, plates, and lock relative motion between the two.

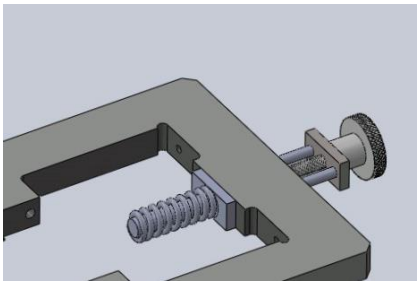

Figure 3.10: CAD Model of Spring, two blocks and guide pins assembly

The position of the knife-edge optical sensor was changed. In the new design, the sensor is attached to the bottom of the moving block approximately at the center. In addition a clamp which holds the knife blade was manufactured. This sensor clamp was mounted on the bottom side of the outer frame. A hole was also drilled through the top surface of the frame, through which a bolt could be placed so as to hold the IR sensor near the knife blade.

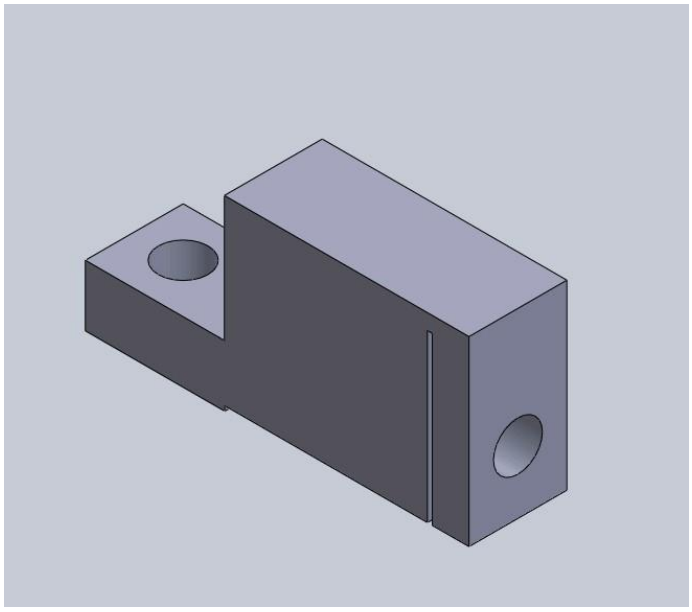

Figure 3.11: CAD Model of sensor clamp

In the new design, the outside frame is in direct contact with the actuator (Aluminum rod) through the pipe nipple adapter. This induces a possibility of change in the dimensions of the frame as well as thermal fatigue. To avoid this a hole was drilled through the frame close to the contact point with the actuator. Cooling liquid passes through this hole to maintain the frame at a constant temperature. Additionally, two holes in the flexure block were drilled to avoid any thermal gradient in the flexure block due to heat exchange between the actuator and flexure block. Another change in the design was that the flexure clamp, which holds the leaf springs, was cut and separated to be individual clamps.

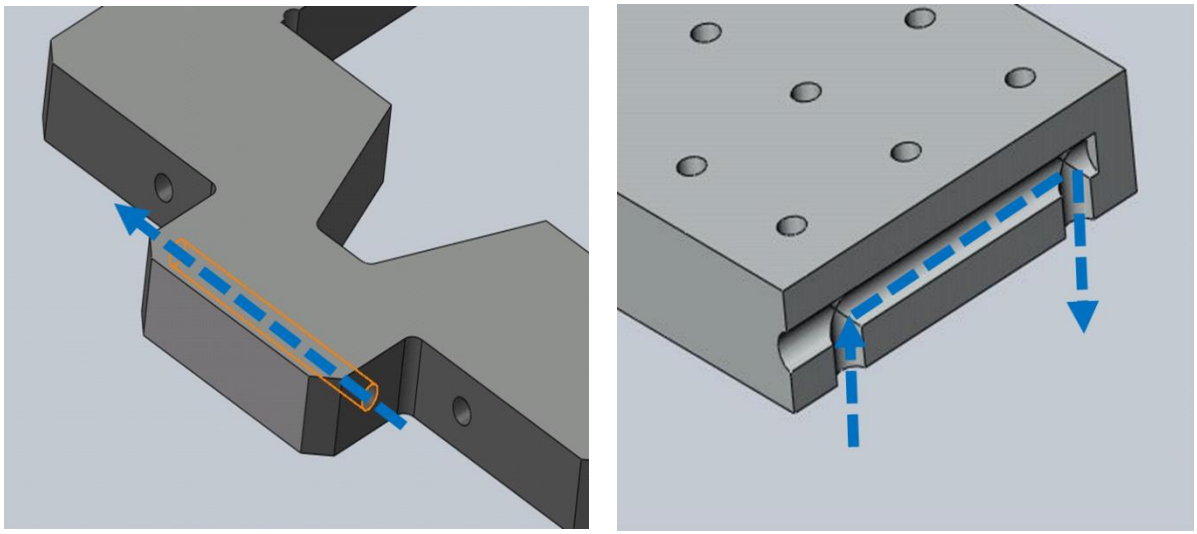

Figure 3.12: Holes on frame and flexure block

There was a possibility that the flexure block may deviate from the intended linear path due to the line of action of the actuator and spring not exactly normal or along the center. The original frame was tested for this deviation using a laser interferometer by mounting it on the Monarch CNC Milling Machine bed in the Metrology Lab of Duke Centennial Hall Room 126.

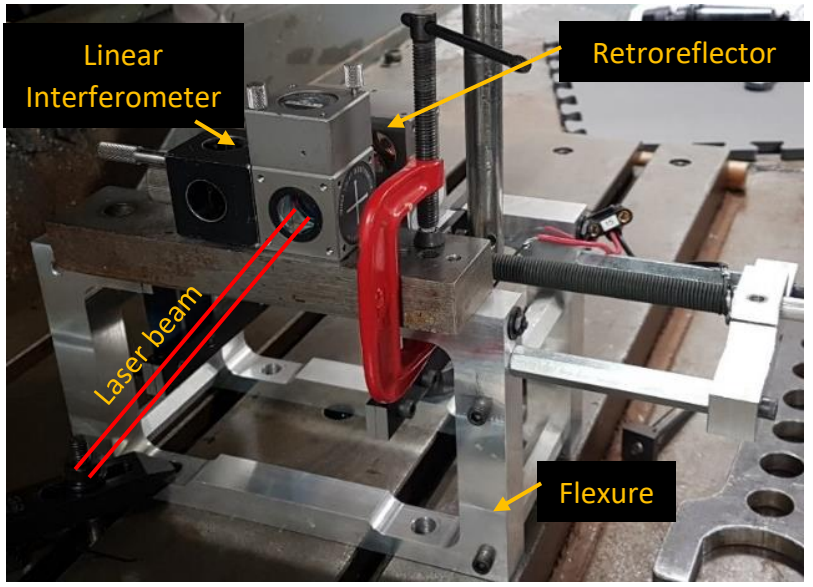

Figure 3.13: Straightness error measurement flexure

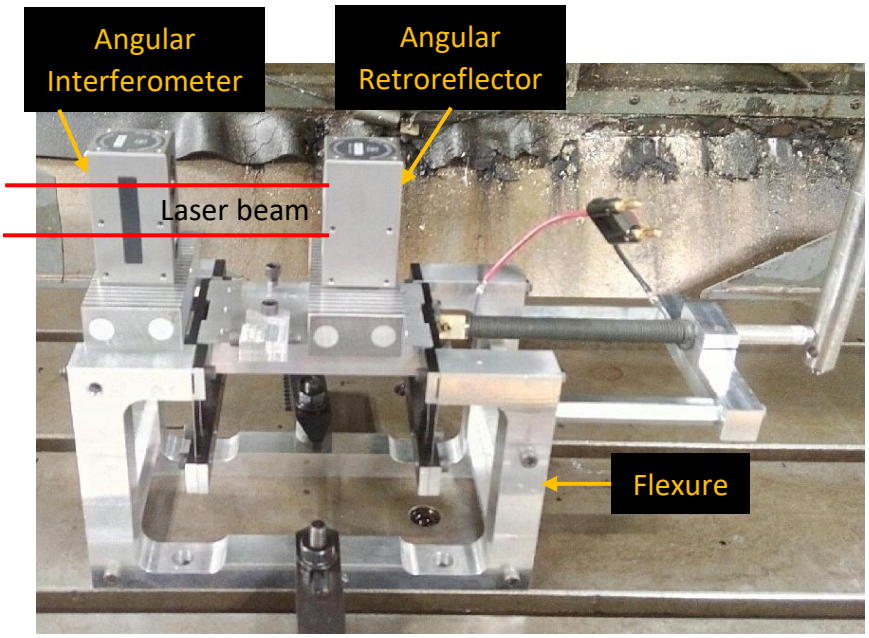

Figure 3.14: Pitch error measurement flexure

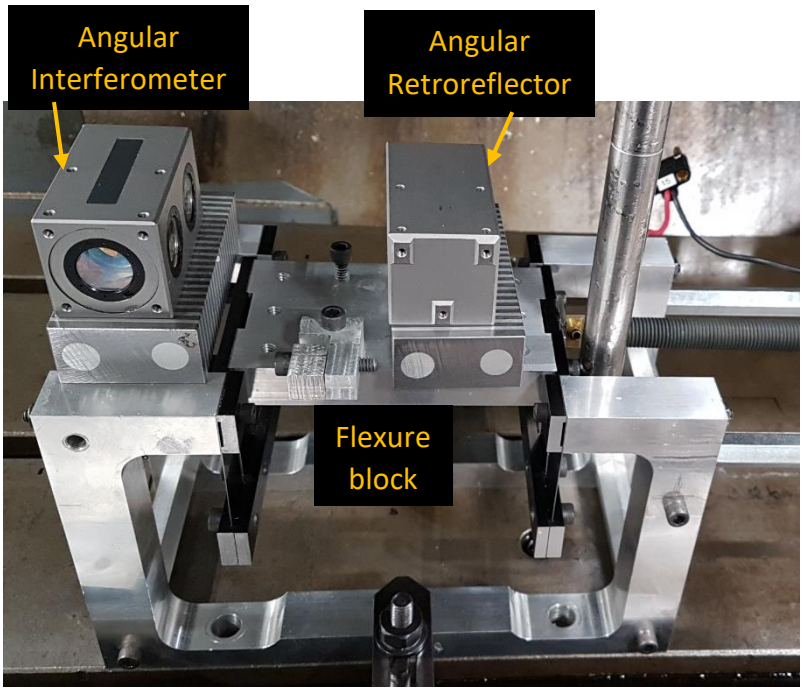

Figure 3.15: Yaw error measurement flexure

From this test, the mean straightness error was found to be 0.122 um, the mean pitch error was found to be 0.54 arc-sec and mean yaw error as 0.62 arc-sec.

Even though the above values are negligible for the original frame, it was difficult to predict the error motion of the flexure block at the design stage. Hence two holes were drilled on the frame's central section while machining, so that four oval guide pins can be inserted to guide the flexure block. This arrangement reduced the possibility for yawing error motion of the flexure.

4. Manufacturing

4.1. Steel frame

Manufacturing of the reinforcing frame was done on a Hass CNC machine due to the complexity of the part profile. The stock 1018 steel plate was 0.75”x8”x24” and cut to approximately 15” in length for the milling operation. The profile of the part was milled using a pocketing tool path with a 0.75” carbide end mill and a finishing pass was made with a 0.25” ball point end mill. A vertical through-hole was drilled on the CNC set-up. The inner profile was enlarged by 0.05” from the initial cut profile on a Bridgeport conventional milling machine using a 0.75” HSS end mill. Holes were drilled on the Bridgeport using a 0.25” extended drill bit, a standard 0.25” drill bit, and other drills to make drawing specifications. Tapped holes were made using 5/16-24 relieved tap and a 1/4-20 HSS tap. Black oxide 10-24 alloy steel socket head screws were used to mount this frame on the existing aluminium base.

Figure 4.1: Steel Plate

4.2. Guide plates (inner and outer)

Both guide plates were manufactured on the Bridgeport conventional milling machine from 0.25”x0.75” high-tolerance mild steel bar stock. Cutting tools used were a 0.75” HSS end mill and specific drills for clearance specifications per part drawings. Dowel pins (guide rods) with 0.25” OD were prepared and clamped using a collect block, allowing for a 1/8” hole to be drilled and reamed at both ends at the holes. The assembly was pressed together using 1/8”x1.25” dowel pins connecting the guide plates to the guide rods.

Figure 4.2: Guide Plate Assembly

4.3. Spring guide

To guide the spring along the desired direction of the applied force and flexure motion, a spring guide was manufactured. The guide was machined on a manual lathe from 0.5” OD aluminium rod stock. On the mounting end of the guide 5/6-24 threads were made to fix it to the frame.

Figure 4.3: Spring Guide

4.4. Knife holder

The knife holder shown in figure 4.4 was used for holding the knife in the knife-edge sensor system. It was machined from stock aluminium material. Holes were drilled using a 0.25” standard drill bit and a #7 standard drill bit. Threads were added as the clamping mechanism using 1/4-20 tap. The knife slot was cut using a fine-tooth band saw.

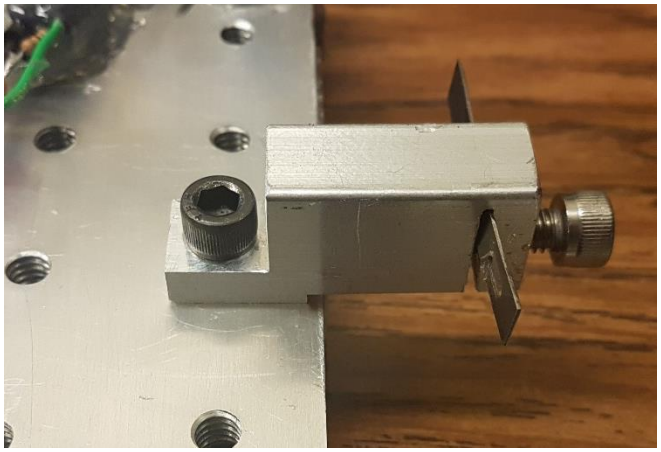

Figure 4.4: Manufactured Knife holder

4.5. Modified parts

4.5.1. Flexure stage

In order to incorporate cooling system, two 0.25” holes 0.375” deep were drilled from the bottom side of flexure stage. Further, to connect these holes together, a horizontal 0.25” hole was drilled from one side. A rubber tube fragment was used to close the entry of the side hole.

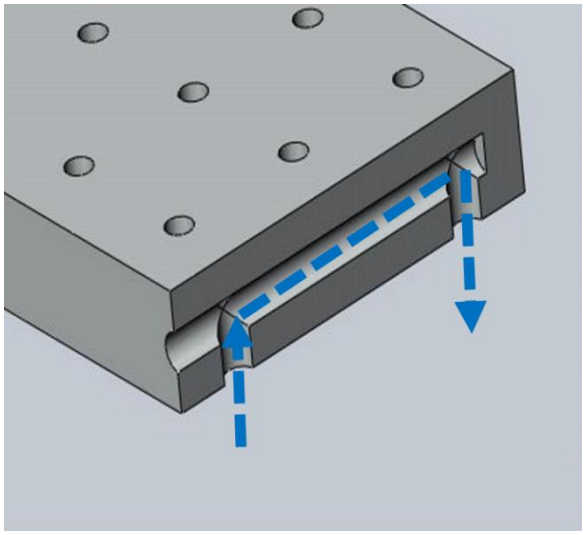

Figure 4.5: Modified flexure stage

4.5.2. Flexure leaf clamps

The flexure clamps were produced by modifying the existing flexure components to fit the new design. The desired leaf spring clamps were made by cutting the existing clamps to size.

Figure 4.6: Flexure Leaf Clamps

4.5.3. Nichrome wire coiling

Nichrome wire, which supplied heat to the actuator, needed to be tightly wound on the actuator in order to have good contact. For this, the actuator was mounted on a lathe spindle. One end of the wire was held fixed, and the other end was clamped to the jaw of the spindle. The wire was coiled around an aluminium rod stock that had been machined to a diameter slightly smaller than the coated actuator tube outer diameter.

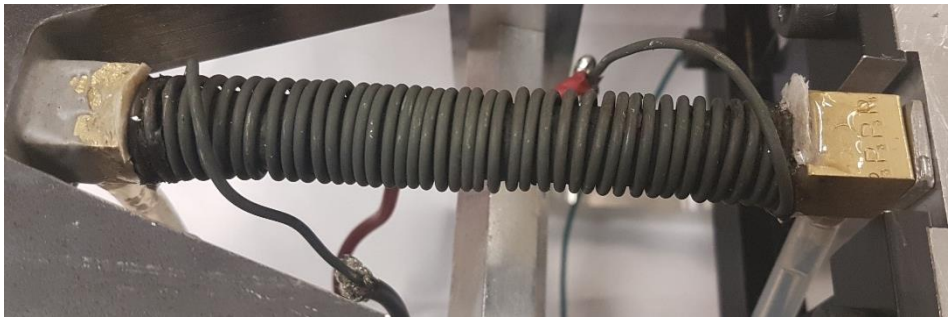

Figure 4.7: Ni-Cr Wire wound on the actuator

5. Bill of Materials

Most of the standard components were procured online from McMaster Carr Website. The rest of the components were either manufactured as explained above or were readily available through stock in Dr. Smith's Lab.

The bill of materials is documented in Table 1. For links to the online components refer Appendix II

Table 1: Bill of Materials

	Item	Part Number	Description	Material	Supplier	Price ea. $	Qty	Total Cost
Frame	Steel Plate	9143K734	0.75'' thick, 8''x24'', 2 ft length	1018 steel plate	McMaster Carr	133.01	1	133.01
	Screw	91251A934	Fastening actuator side for frame, 10-24 thread,5"1/2" lg.	Black-Oxide Alloy Steel	McMaster Carr	3.19	2	6.38
	Screw	91251A260	Fastening spring side of frame, 10-24 thread, 4 3/4" length	Black-Oxide Alloy Steel	McMaster Carr	2.96	2	5.92
	Washer	90107A011	Flat type washer with ID 0.203", OD 0.438", Thickness 0.024"-0.038"	316 Stainless Steel	McMaster Carr	4.24	1	4.24
	Hex Standoff	91780A245	5/8" OD, 1/4"-20 , 3 1/2" length, Female thread	2011 Aluminum	McMaster Carr	3.36	1	3.36
	Nut	91841A011	10-24, 1/8" thick, pack of 100	18-8 Stainless Steel	McMaster Carr	3.50	1	3.50
Actuator	Steel drive tube	4830K116	NPT Male Threaded on Both Ends, 1/8 Pipe Size, 4" Long	304/304L Stainless Steel	McMaster Carr	3.18	1	3.18

Actuator	Aluminum drive tube	44665K117	NPT Male Threaded on Both Ends, 1/8 Pipe Size, 4" Long	Aluminum	McMaster Carr	2.08	1	2.08
	Brass hose barb	WP7362568	1/8 FNPT, 1/4" tube size, barbed, 90deg elbow	Brass	Grainger	4.34	4	17.36
	Guide rods (flexure stage)	8890K183	0.1990" OD 3 ft. 6 ft.	Tool Steel	McMaster Carr	6.50	1	6.50
	Set screws	92765A311	Oval tip, 1/4"-20 thread size, 1" length, Hex Coarse thread set screws	Alloy Steel	McMaster Carr	10.17	1	10.17
	Guide pins (compression screw)	98381A554	1/4" OD, 3" length, dowel pin	Hardened Alloy Steel	McMaster Carr	8.03	1	8.03
	Knurled-Rim Knob	6079K33	5/16"-24 x 1-3/4" Threaded Stud, 1-1/2" Diameter	Black-Oxide Steel	McMaster Carr	5.59	1	5.59
	Compression Spring	9657K399	Zinc-Plated, Music-Wire, Closed & Flat Ends, 2" Long, 3/4" OD, 294 lb/in	Zinc-Plated Music-Wire Steel	McMaster Carr	1.71	10.3	17.61
	Steal bar stock	9517K433	1/4" thick, 3/4" wide, 2 ft length rectangular bar	Low-Carbon Steel	McMaster Carr	20.34	1	20.34
	Aluminum shaft stock	-	15" OD (for spring guide)	6061 Al	Lab Stock		1	
	Ni-Cr wire	8880K11	0.064" Diameter, 1/4 lb. Spool, 21' Long	Nickel Chromium	McMaster Carr	21.28	1	21.28
Cooling and isolation	Round Seal	12975K35	O-Ring Cord Stock, 1/4" OD, 3' length.	Neoprene Rubber	McMaster Carr	1.65	1	1.65
	Plastic tubing	51135K16	Durometer 50A, 1/8" ID, 1/4" OD, 375F, 10ft	Silicone Rubber	McMaster Carr	0.69	10	6.9
	Plastic tubing	-	Cooling Pipes	PVC	Lab Stock	-	-	-
	Glass	-	For low friction surface for guide rods against flexure	Glass	Lab Stock	-	-	-
Controls	myRIO	-	Controller	-	Lab Stock	-	1	-
	16 bit ADC	-	Analog to Digital Converter	-	Lab Stock	-	1	-
	12V 10A power supply	-	TDK Lambda	-	Lab Stock	-	1	-

Controls	Power amplifier	-	Amplifier	-	Lab Stock	-	1	-
	± 12 V Power supply	-	RIGOL Power Supply	-	Lab Stock	-	1	-
	Temperature sensors	-	LM 35	-	Lab Stock	-	2	-
	Optical Sensor	-	RPI 0352E	-	Lab Stock	-	1	-
	TOTAL						**$ 277.10**	

6. Control System:

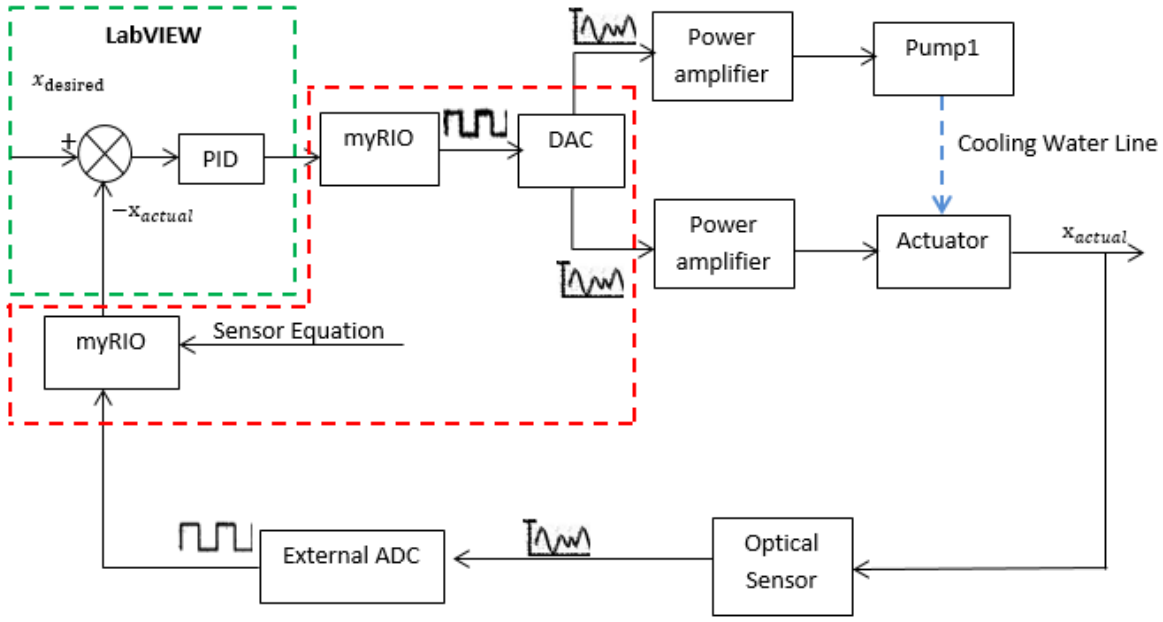

Figure 6.1: Block Diagram of the new Control System

In the original design, as described before, the pump and heating element were wired to the Arduino Uno through a motor driver. The motor driver regulated the power given to either the pump or the heating coil by pulse width modulation. Power supply was connected as inlet to the motor driver and output channels were connected to the pump and to the heating element. [1]

In the revised design, the Arduino Uno is replaced by myRIO as it has onboard FPGA ('field-programmable gate array), which is an IC that can be configured after manufacturing, allowing high-speed data acquisition/filtering/logic/digital IO on the order of 40 MHz, which is much faster than the Arduino. Also, it was run using LabVIEW GUI [4]. The myRIO was connected to LabVIEW software installed on the computer through a USB interface. LabVIEW has a built-in PID algorithm, which reads the error between the desired position and current position of the flexure. This input was compared with

the feedback received from the optical sensor. The output of the PID is then sent to an external Digital to Analog converter, which converts digital signals to analog. As the amplitude of the analog signal is too weak to run the 12 V cooling water pump independently, the signal is amplified using an amplifier connected to a +- 5V AAK Corporation power supply. There are two pumps, one connected to the actuator and another one connected to the outer frame and flexure block. The pump controls the flow rate of cooling water through the cooling pipes.

The heating coil wound around the actuator was connected to constant 12V/10A power supply made by TDK Lambda. By controlling the cooling water flow rate through the pipes, we can control the temperature of the actuator. Thus, we can control the expansion or contraction of the actuator. The current position due to change in length is measured by the RPI 0352E optical knife-edge sensor which is connected to a 15V RIGOL Power Supply. This optical sensor gives a voltage output, which is proportional to the penetration of the knife-edge into the sensor. The output voltage was then sent to the myRIO through an external 16-bit Analog to Digital Converter run by myRIO. Depending upon this feedback and the desired position input, by changing the cooling rate we can reach the desired configuration.

7. Testing

Testing verifies whether the system meets the different requirements including functionality, performance and reliability. In order to evaluate the performance of the modified design of flexure system, dynamic and thermal tests were performed. Procedure and results of these tests are as follows.

7.1. 100 micrometer displacement test

Industrial application of flexural system demands high load bearing capacity. For example, a precision tool holder operated using flexures for precisely positioning a single point cutting tool in lathe machine. Hence, the purpose of the test was to determine whether the actuator could displace the flexure to its maximum desired range of 100µm and system stability against the applied variable preload.

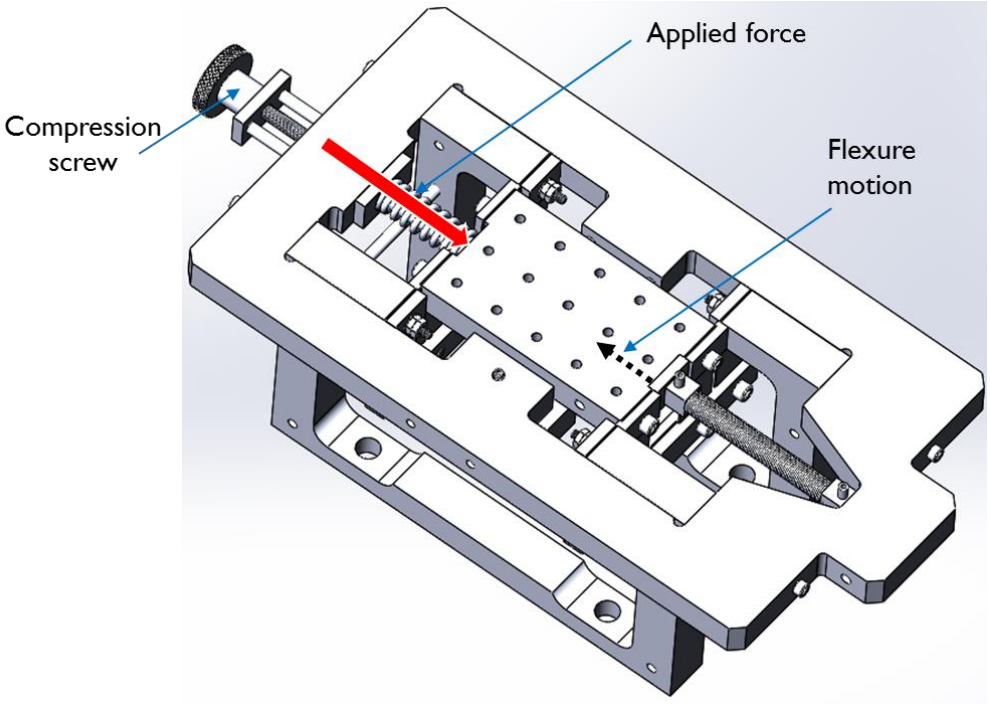

Figure 7.1: 100µm displacement test

Procedure:
Variable load of 0 N to 1000 N with an increment of 100 N was applied on the flexure through compression spring. The actuator was heated with the nichrome coil which displaced the flexure to 100µm position against the preload.

Equipment:
Calibrated Infra-red sensor and the sensor knife (mounted on flexure frame) were used to track the motion of the flexure

Results:
After performing the test, it was found that the actuator is able to displace the flexure up to 100 µm under each applied load. The time constant was evaluated for 100 µm displacement under 0N and 500N.

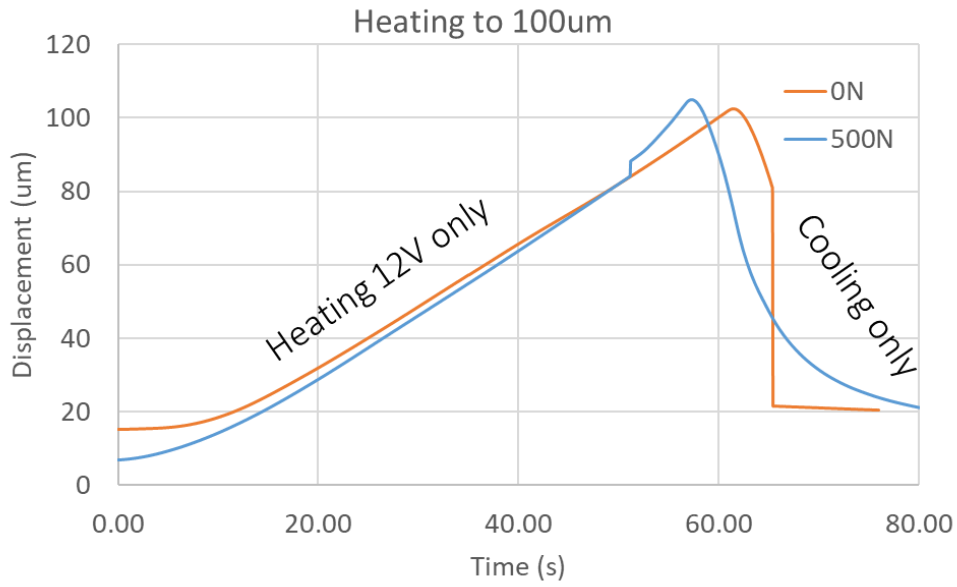

Figure 7.2: 100µm displacement test result

Figure 7.2 shows the displacement of actuator under 0N and 500N. Heating time constants under **0N load** and **500N load** was found to be **60 seconds** and **55 seconds** respectively. On the other hand, cooling time constants under **0N load** and **500N load** was found to be **15 seconds** and **25 seconds** respectively.

When the actuator was allowed to expand beyond 100 µm, it was able to reach up to **200 µm** in **60 seconds** under **500N** and **65 seconds** under **1000N** respectively from its 100µm position. The results are shown in the figure 7.3.

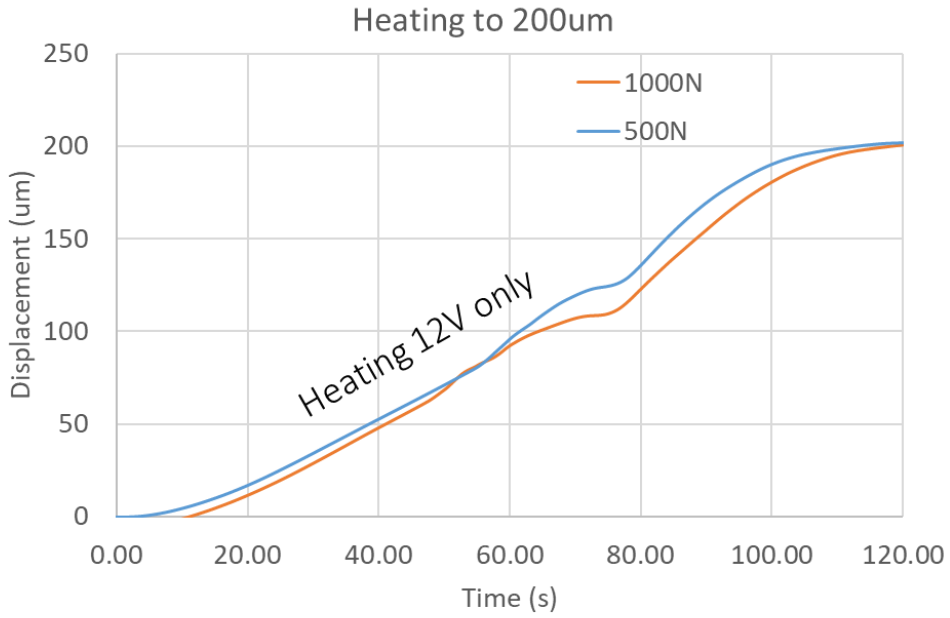

Figure 7.3: 200µm displacement test result

7.2. Incremental displacement test

Along with the high load carrying capacity, movement of the flexure should be precise and accurately match the commanded position. In this test, positional accuracy of the flexure was analysed.

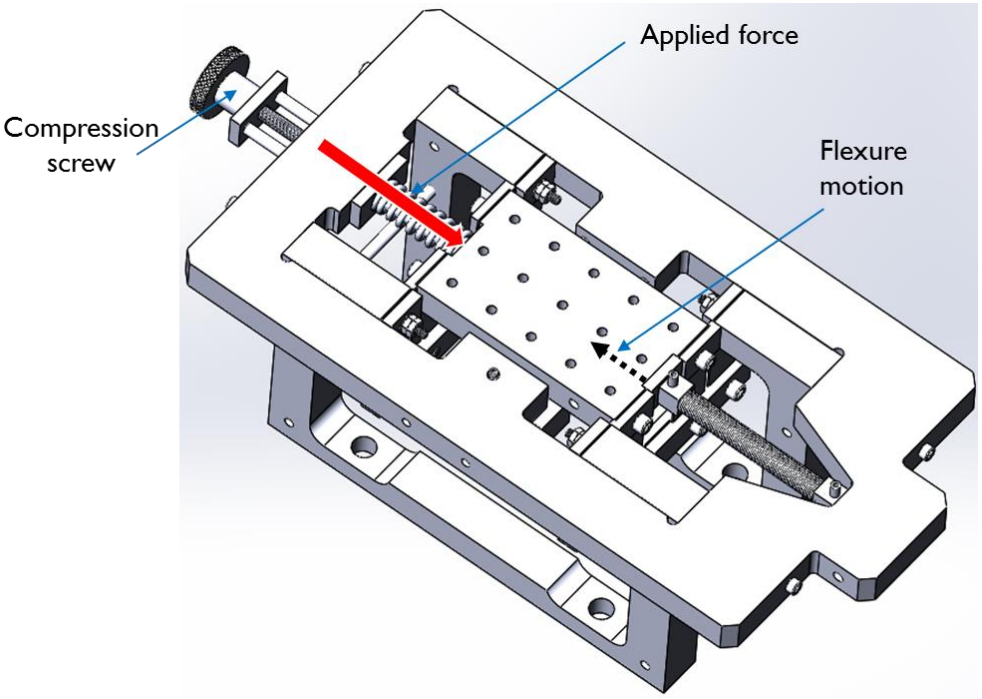

Figure 7.4: Incremental displacement test

Procedure:
In this test, unlike the previous one, the preload value was kept constant and the actuator was allowed to move from 0 µm to 100 µm (which is the full range) with an increment of 10 µm. At each position, the actuator motion was checked against the commanded value. In order to consider repeatability, the same procedure was repeated with preloads of 0 N, 500 N and then 1000 N.

Equipment:
Again, the Calibrated Infrared sensor and the sensor knife (mounted of flexure) were used to track the motion of the flexure.

Results:
Initially the test was done under 0N preload. Figure 7.5 shows the graph of the commanded position and the actual position reached by the actuator.

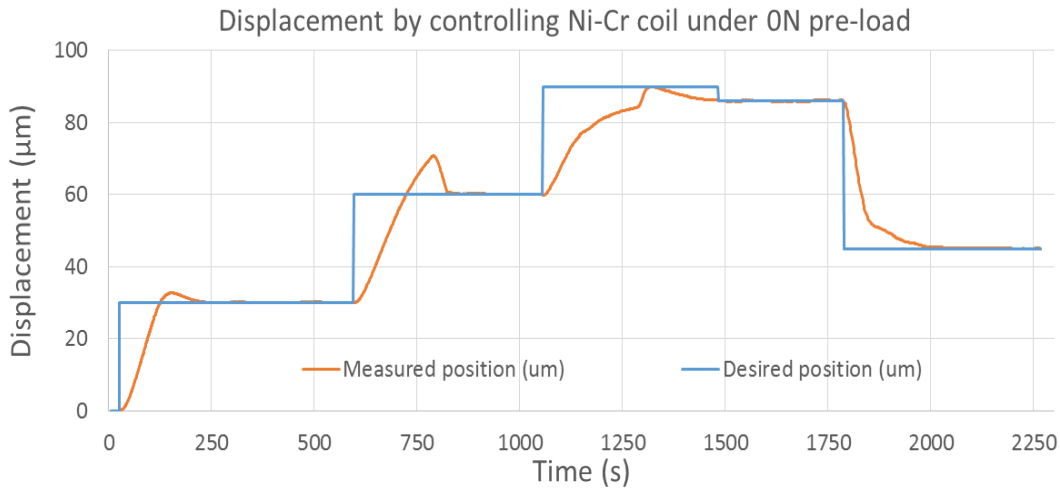

Figure 7.5: Displacement control test under 0N load

The difference between the commanded position and actual position gives the error between them. Figure 7.6 shows the error between commanded position and the actual position reached by the actuator. We can see that error goes on reducing till the system stabilizes at a desired position.

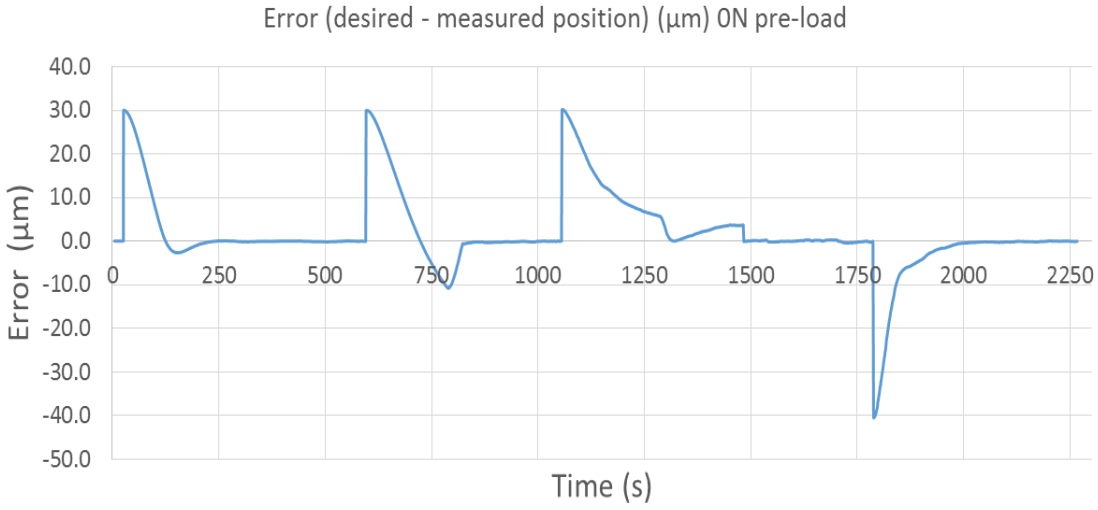

Figure 7.6: Error in the displacement under 0N load

In the same test, we are keeping track over the temperature of the flexure stage and frame. From the figure 7.7, we can see that temperature is controlled. **Variation in the temperature was ± 1 ℃** while the room temperature was 23℃.

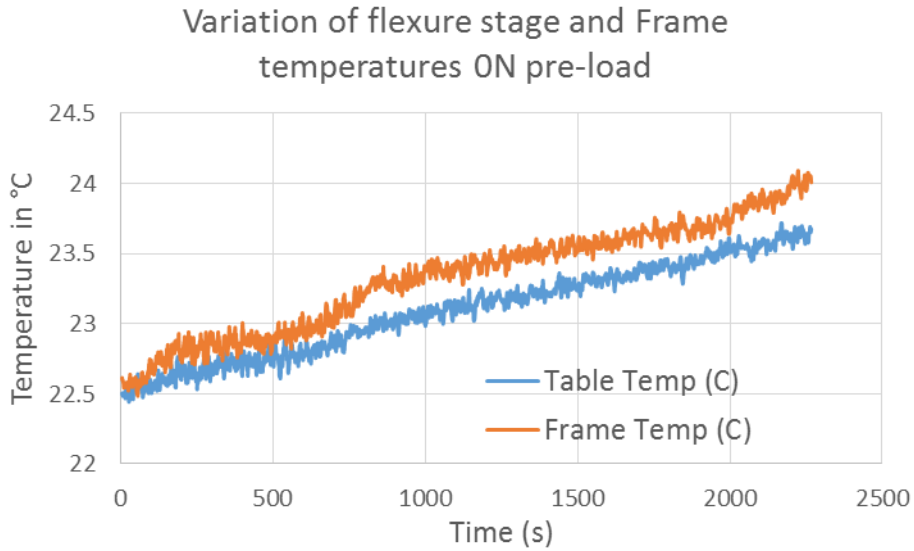

Figure 7.7: Variation in the flexure stage and frame temperature under 0N load

The same test was repeated by changing the preload value to 500N. Figure 7.8 ,7.9 and 7.10 belongs to results of test under 500N load.

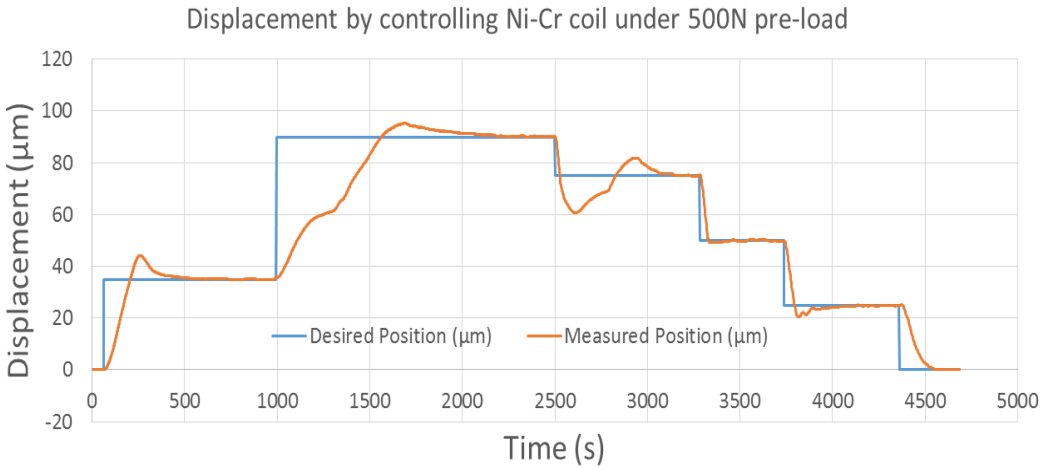

Figure 7.8: Displacement control test under 500N load

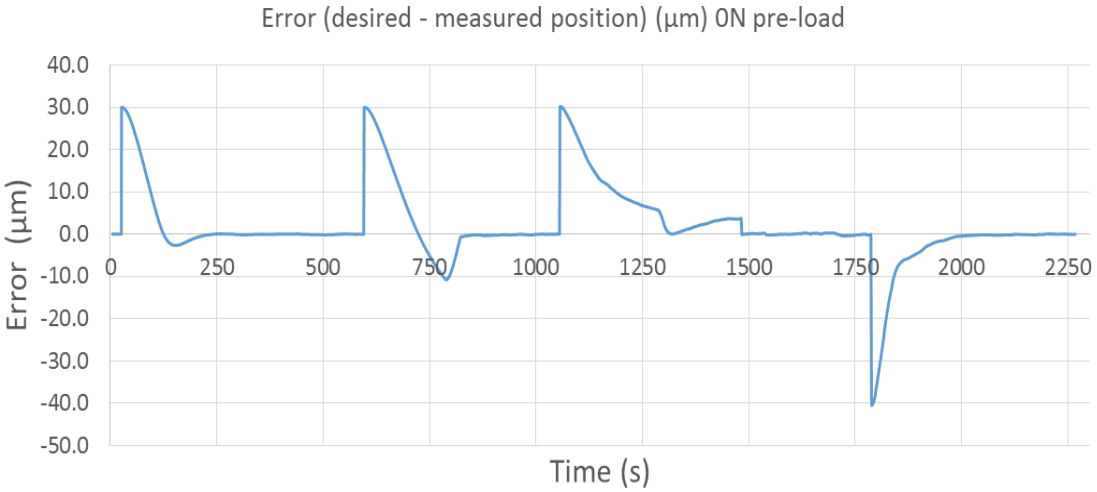

Figure 7.9: Error in the displacement under 500N load

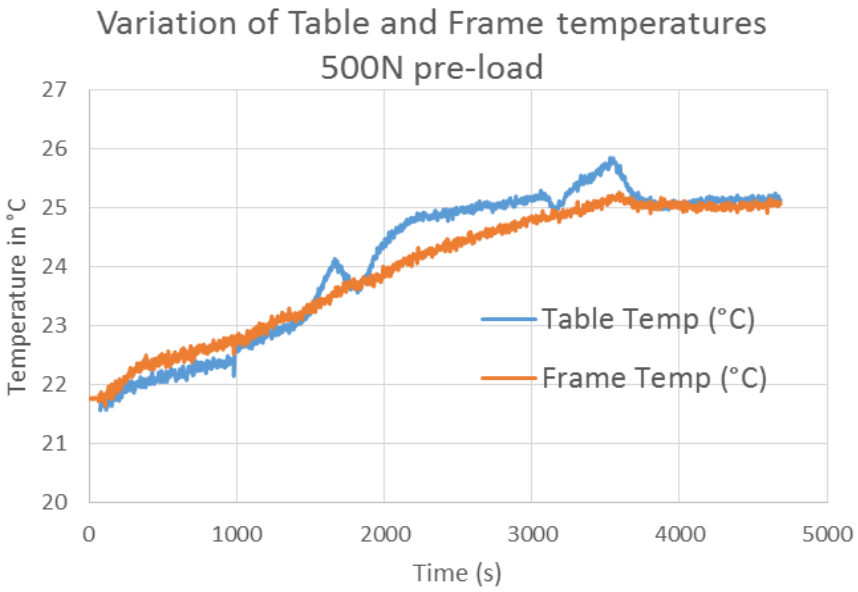

Figure 7.10: Variation in the flexure stage and frame temperature under 500N load

Figure 7.11, 7.12 and 7.13 represents results of test under 1000N load.

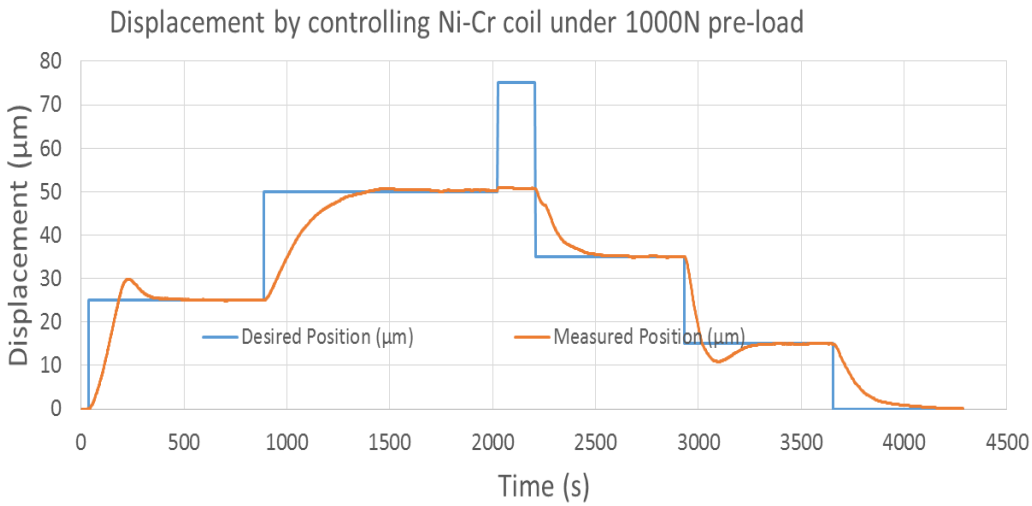

Figure 7.11: Displacement control test under 1000N load

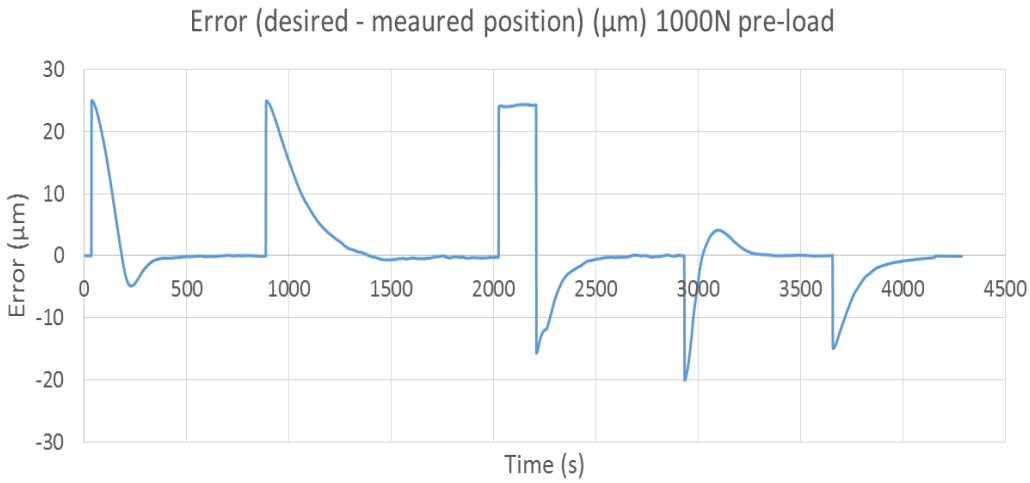

Figure 7.12: Error in the displacement under 1000N load

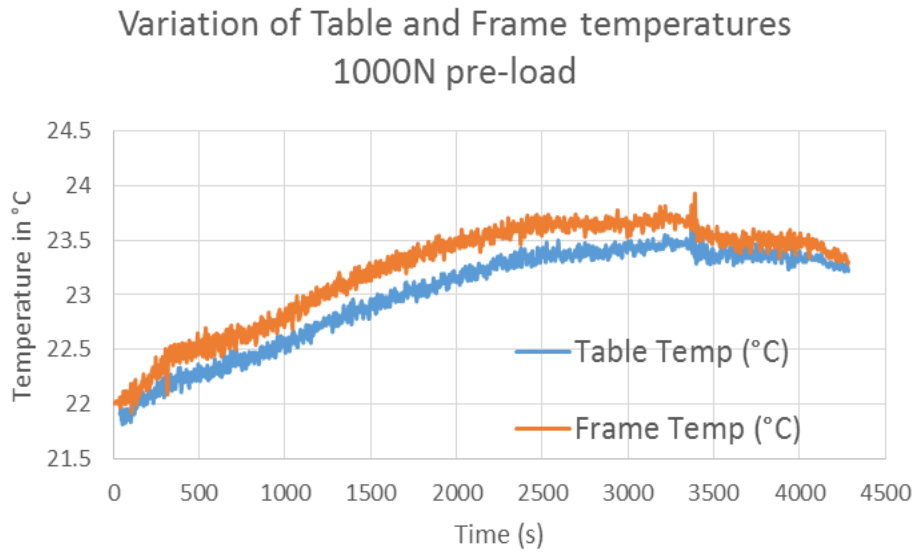

Figure 7.13: Variation in the flexure stage and frame temperature under 1000N load

On zooming in on the response of the actuator displacement, even under 1000N load, the system was observed to be stable once the desired position was reached.

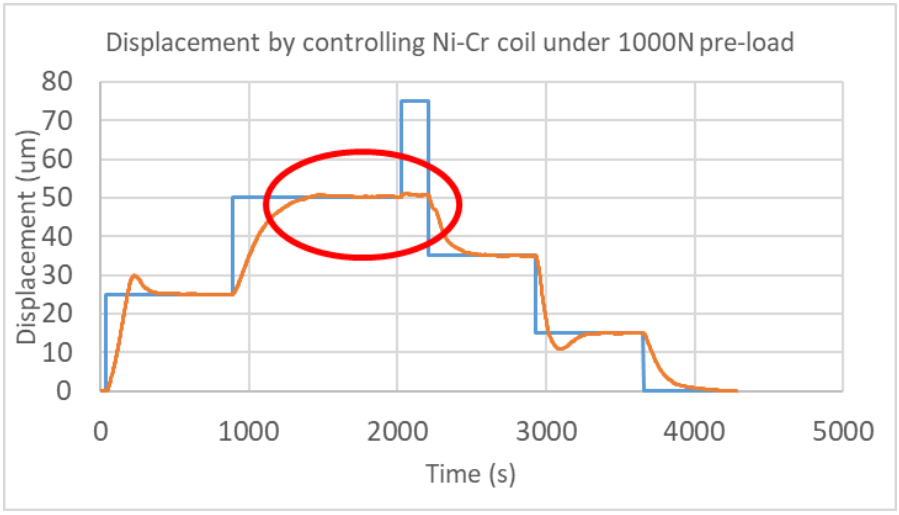

Figure 7.14: Displacement control test under 1000N load

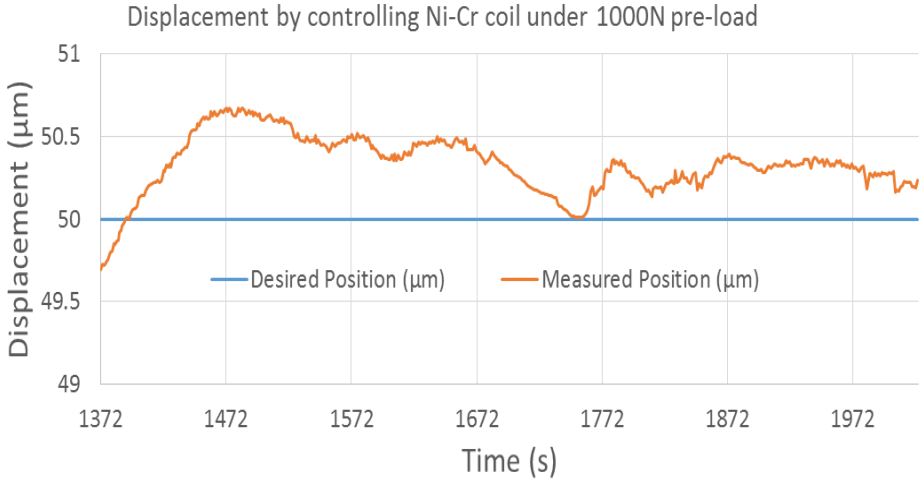

Figure 7.15: Enlarged view of displacement

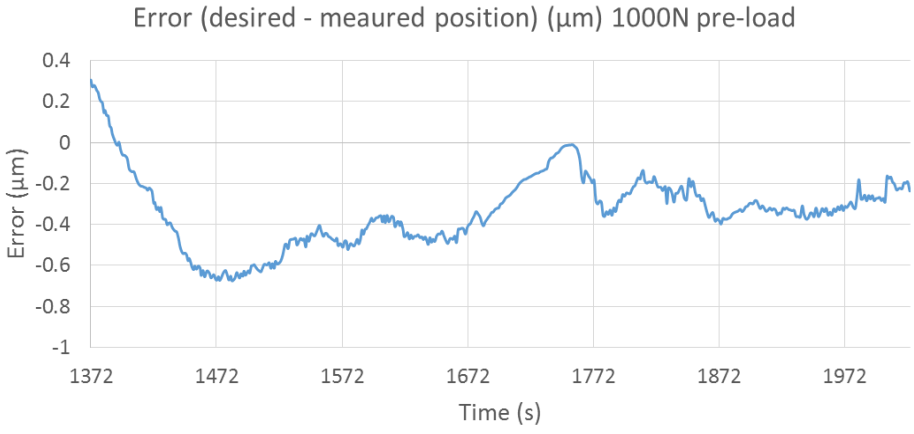

Figure 7.16: Error in the displacement at equilibrium

From the above graphs, we can see that the system takes time to stabilize at given desired position, but after reaching desired position, the error reduces. **Average error** was found to be **0.33 µm** approximately. So, we can say that the system is capable of holding the desired position effectively.

7.3. Test to find heating time constants:

This test was carried out to identify how fast the system is able to reach a desired position. Time constant, i.e. the time required to reach a particular position, 0µm to 30 µm under each 0N, 500N and 1000N preload was evaluated.

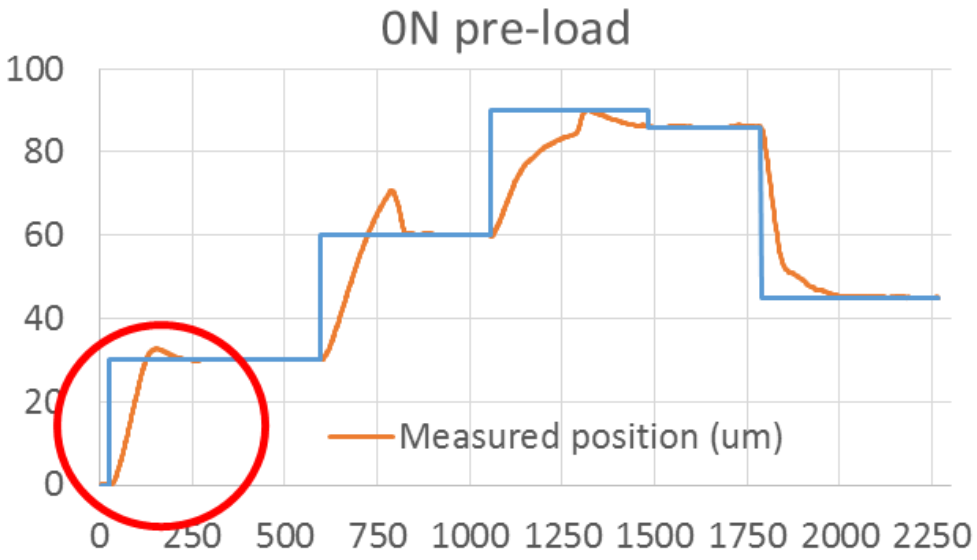

Figure 7.17: Heating time constant at 0N pre-load

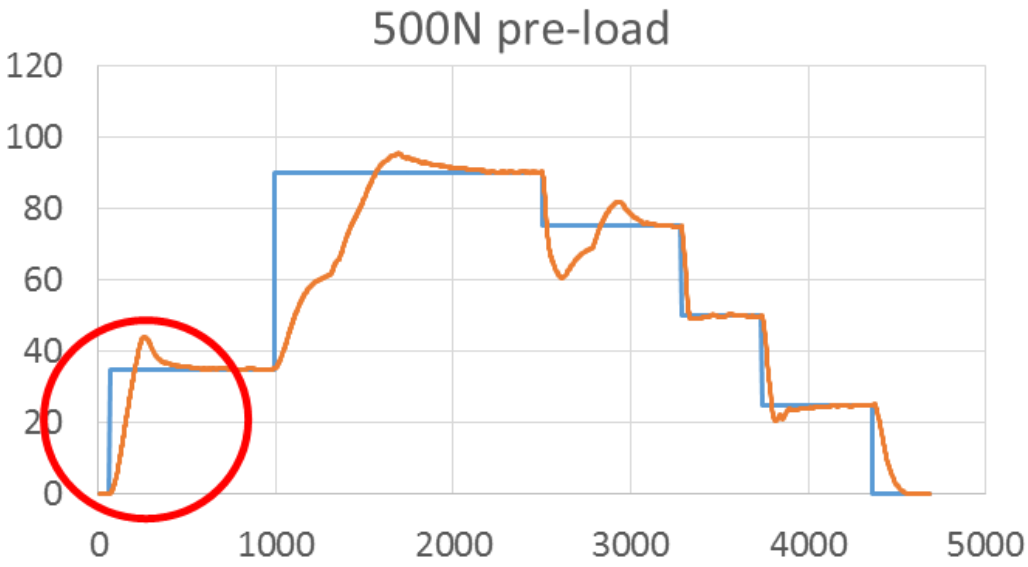

Figure 7.18: Heating time constant at 500N pre-load

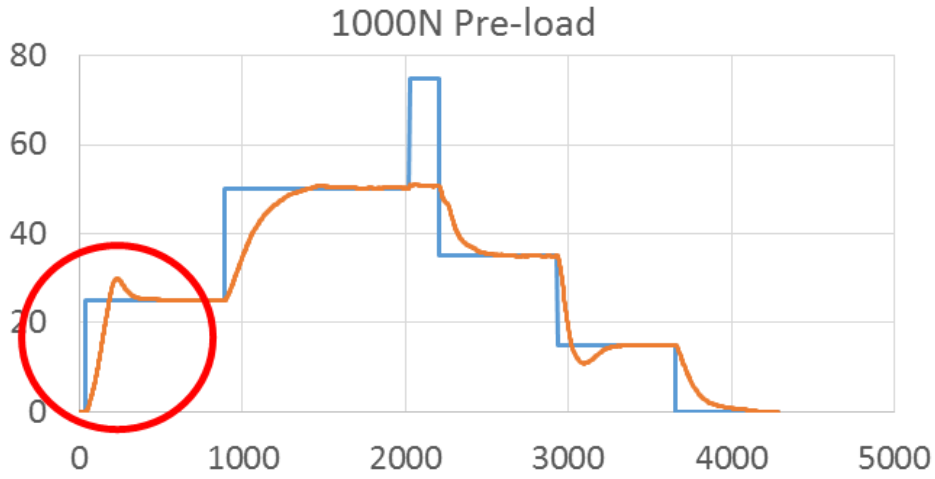

Figure 7.19: Heating time constant at 1000N pre-load

From the figure 7.17, 7.18, 7.19 time required to achieve **30µm** displacement was found out to be **235.2 seconds** under **0N**, **578.6 seconds** under **500N** and **535.1 seconds** under **1000N**. It was seen that time constant under 500N load is greater than time constant under 1000N load. This may be because of friction due to guide pins applying force horizontally.

7.4. Thermal isolation test

The actuation system of the flexure was based on simultaneous heating and cooling to provide controlled motion. When the actuator was heated with a nichrome coil, there was the possibility that the surrounding area would be heated, because of the conduction and convection. In order to prevent thermal expansion of parts other than actuator, cooling water system was used to thermally isolate the actuator. To check the thermal isolation of the system, the following test was performed.

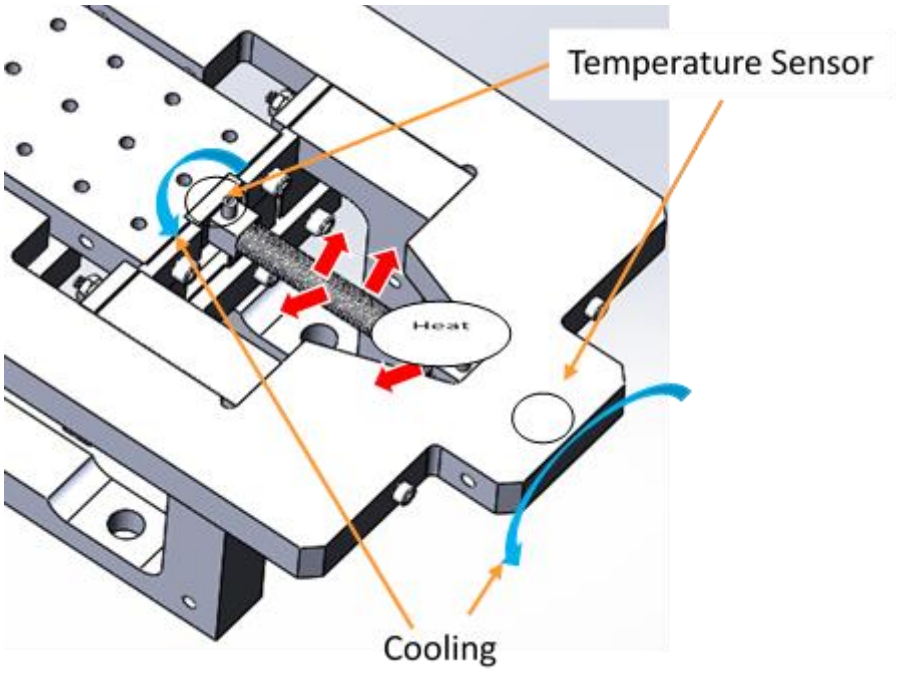

Figure 7.20: Thermal isolation test

Procedure:
The actuator was heated over the working temperature range. The cooling system was turned on. The temperature sensors mounted on the frame and the flexure block were used to measure the temperature at certain locations. The flexure had a 200 N preload and the time was recorded for the actuator to expand and move the flexure 100 µm.

Equipment:
Thermal Sensors, multimeter, power supply

Results:

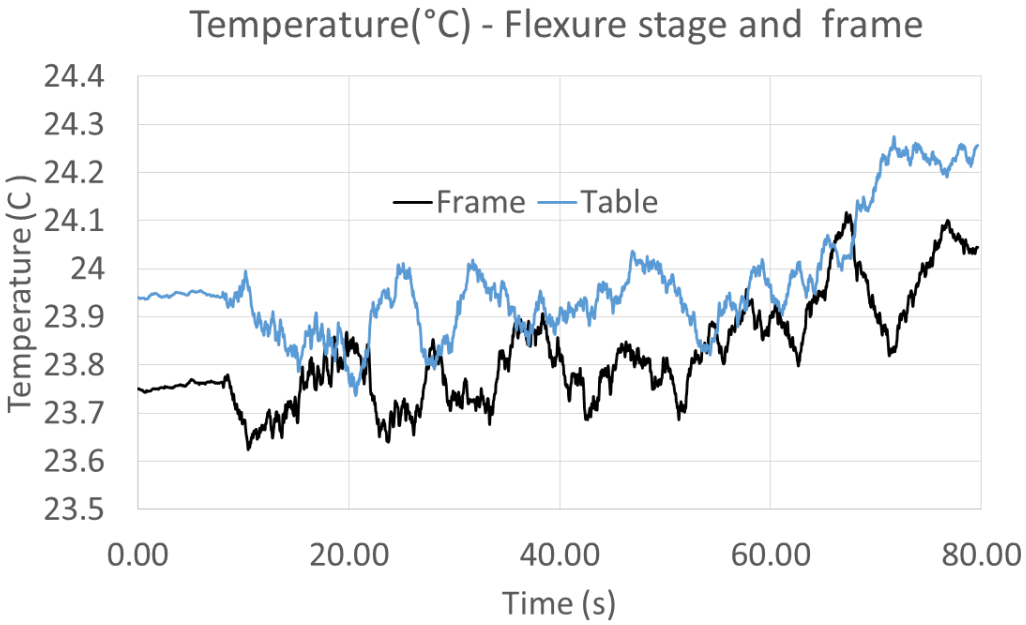

Figure 7.21: Temperature of Flexure stage and frame

A rise of **0.4212 ℃** in the **frame temperature** and **0.5188℃** in the **flexure stage** measurement was observed. The small magnitude of the temperature rise indicates good thermal stability. This proves the effectiveness of water cooling system for thermal isolation of the system.

8. Conclusion

The original flexure stage was modified to increase the load capacity to 1000 N with 100μm range. Even though on changing the load or the displacement, the system is overshoots and eventually reaches a nearly steady state condition. The low magnitude of fluctuations (0.33 μm) obtained at a desired position show the flexure's steady state capability. The flexure can cover its full displacement range in approximately 60 seconds depending upon the pre-load applied and can even cover double its intended range (200μm) in additional 60 seconds. The time obtained was found to be quite satisfactory taking the slow response of thermally actuated flexures in general. The increase in temperature of the surrounding frame and flexure stage both of which are in contact with the actuator was found negligible (0.4212 ℃ and 0.5188℃). This is due to the efficient cooling system employed. The projected goals set at the beginning of the project were successfully completed.

Appendix I: Drawings of Manufactured Components

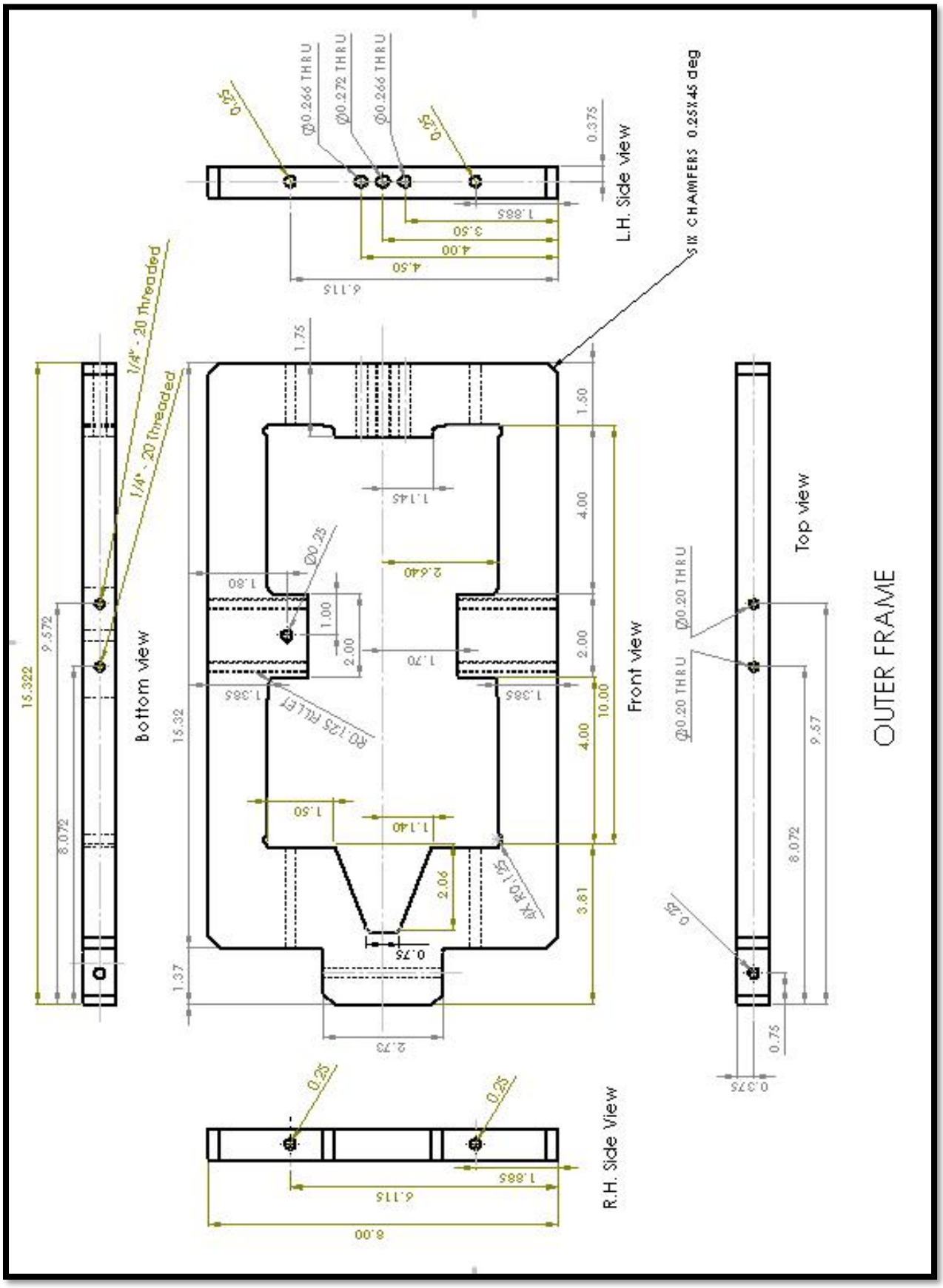

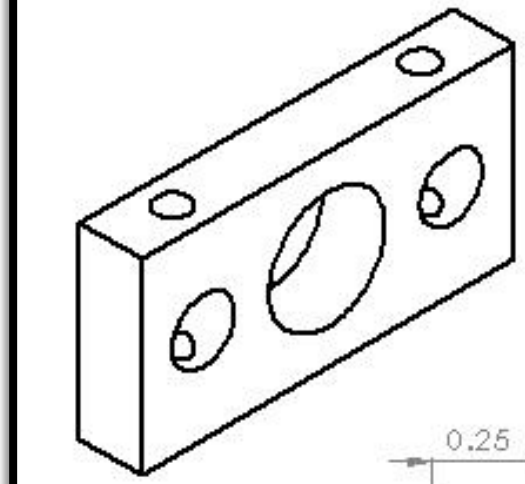

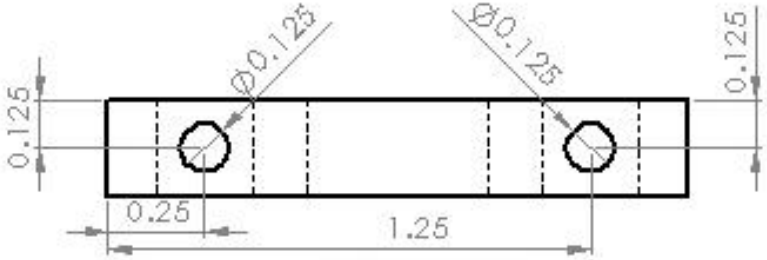

FRONT VIEW

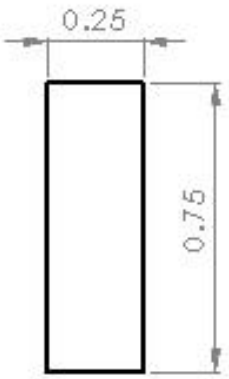

R.H.S VIEW

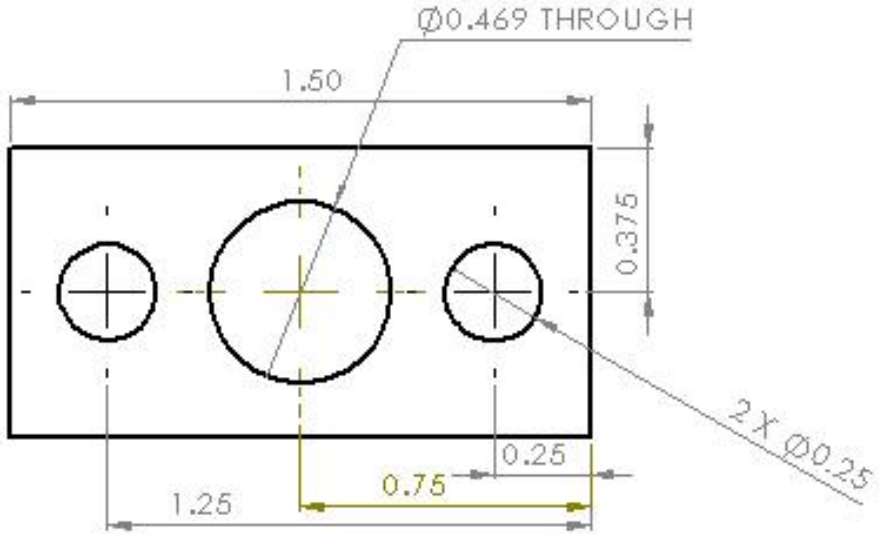

TOP VIEW

GUIDE BLOCK -1

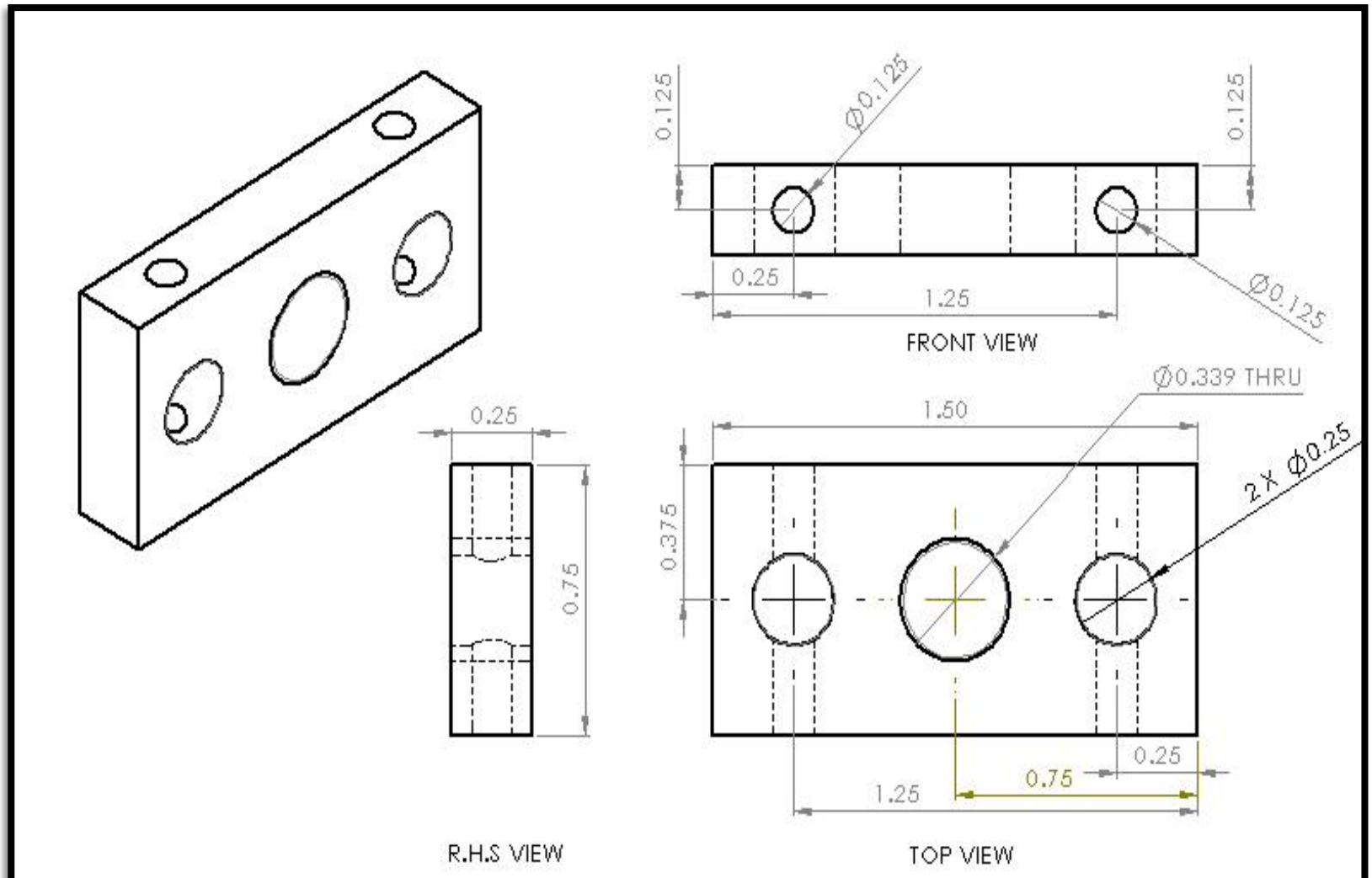

GUIDE BLOCK - 2

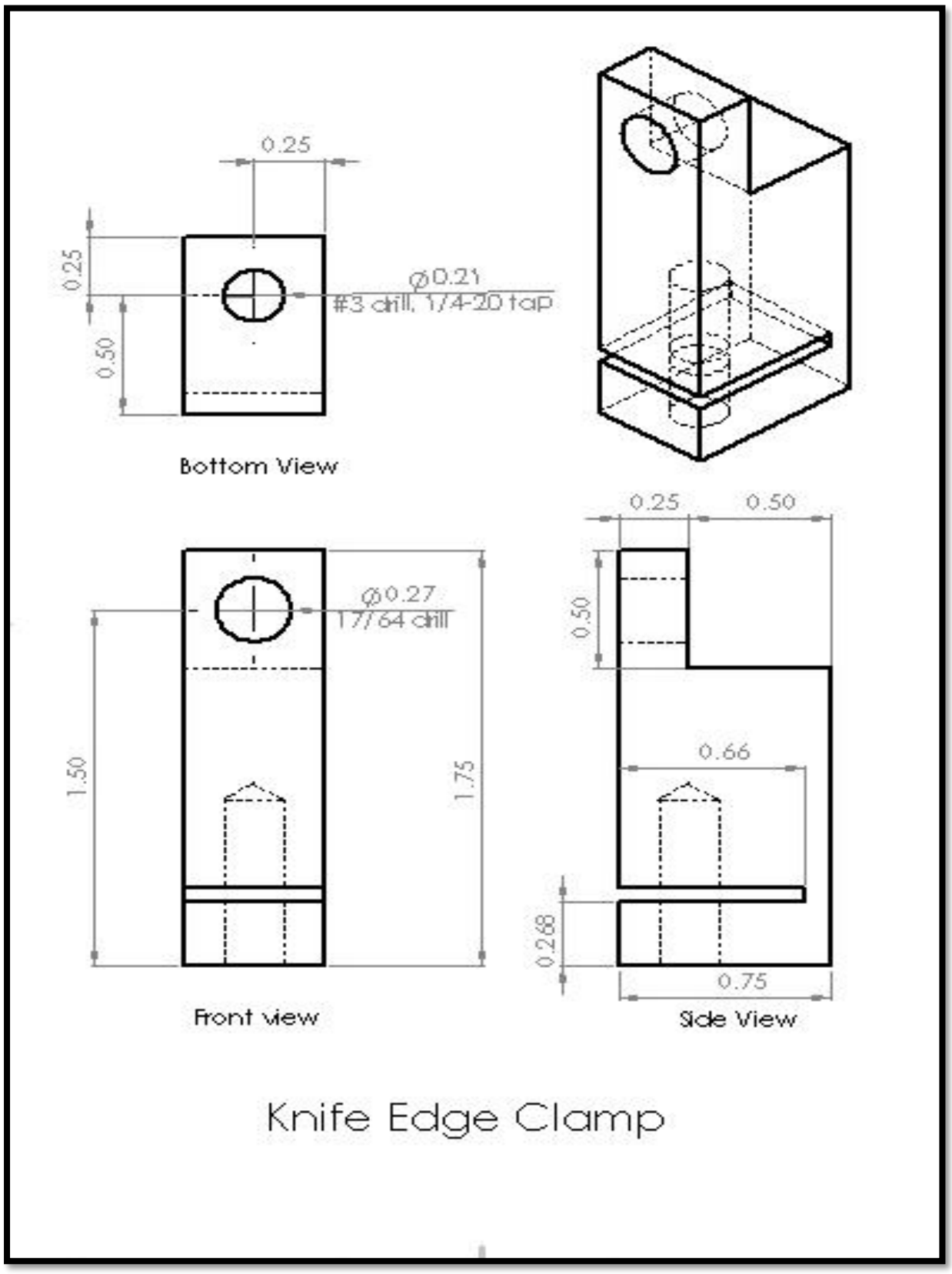
0.25
0.25
0.50
Ø0.21
#3 drill, 1/4-20 tap
Bottom View
0.25
0.50
Ø0.27
17/64 drill
1.50
1.75
0.50
0.66
0.268
0.75
Front view
Side View
Knife Edge Clamp

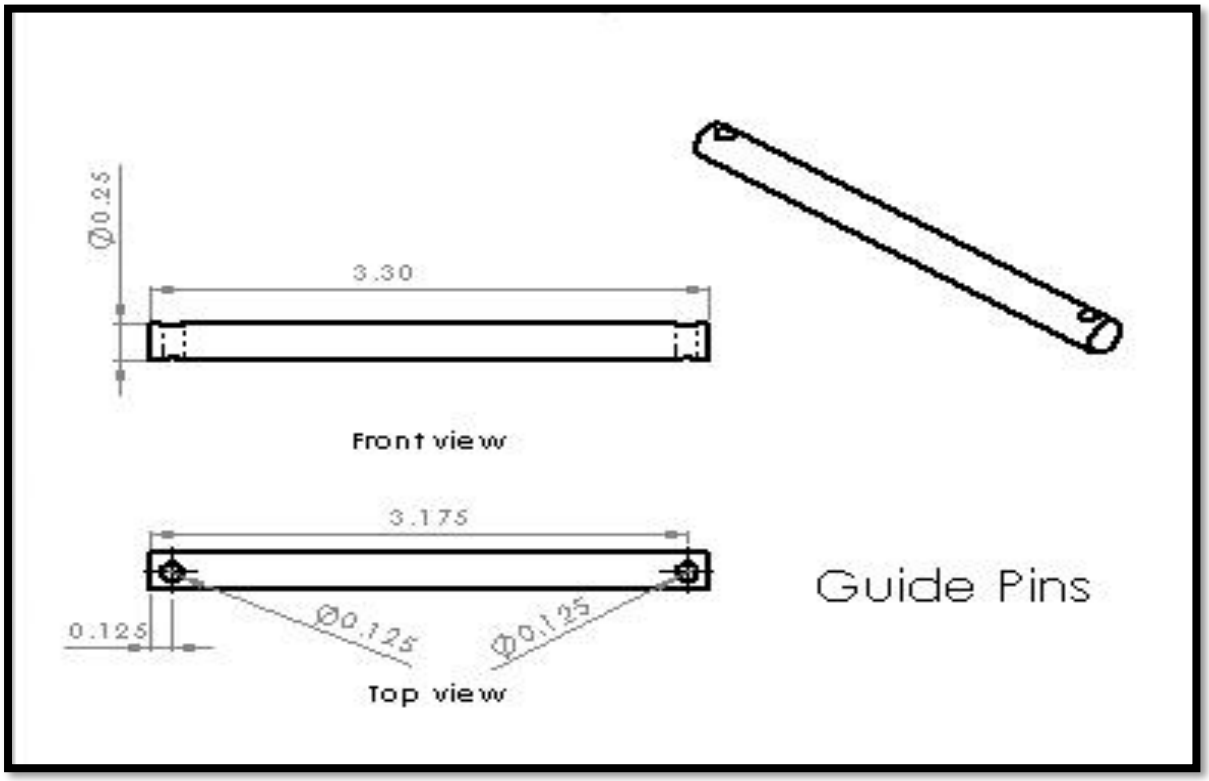
Ø0.25
3.30
Front view
3.175
0.125
Ø0.125
Ø0.125
Top view
Guide Pins

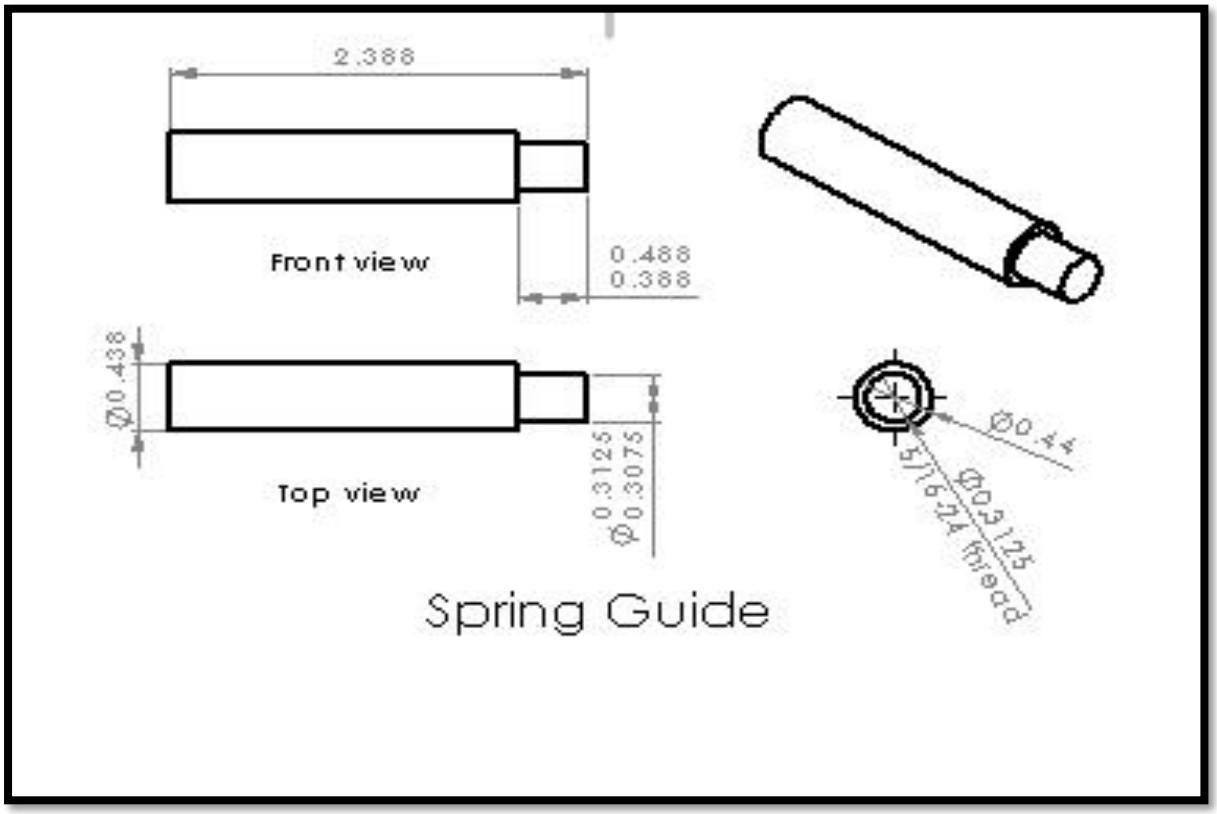
2.388
Front view
0.488
0.388
Ø0.438
Top view
0.3125
Ø0.3075
Ø0.44
5/16-24 thread
Ø0.3125
Spring Guide

The modifications have been dimensioned; the repeated hole pattern already exists.
A hole is created on the side of the block.
Two holes are created originating from the block's underside, and intersect the hole coming from the side.

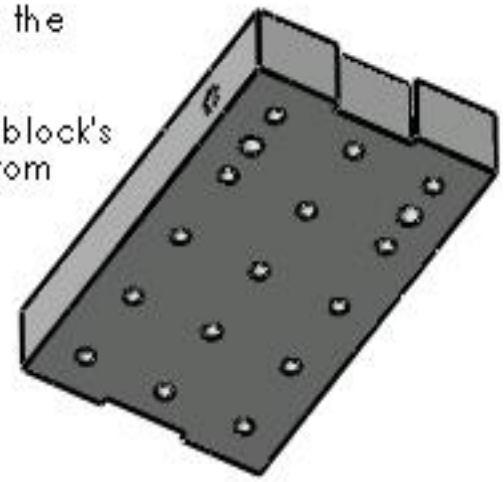

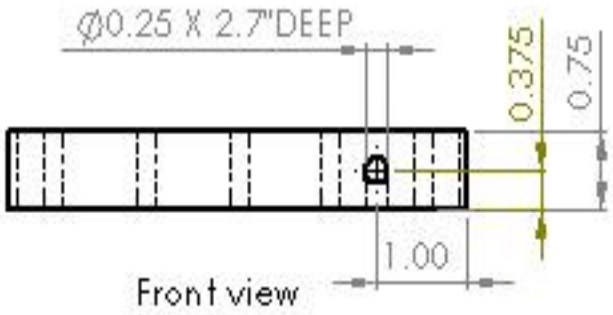

Front view

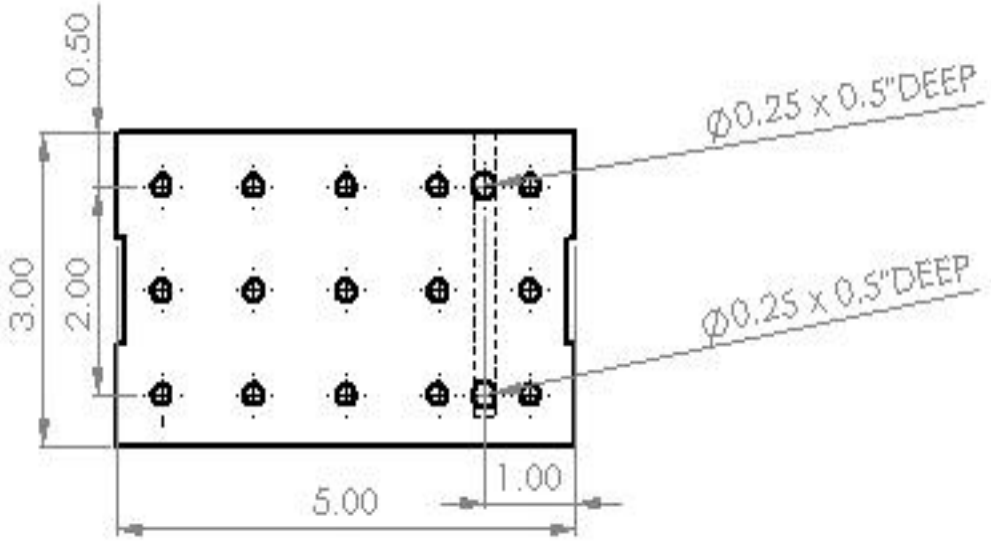

Top view

Flexure stage modification

Appendix II: Bill of materials with links to parts ordered online

Item	Part Number	Website
Steel Plate	9143K734	https://www.mcmaster.com/#9143k734/=16twcmk
Screw	91251A934	https://www.mcmaster.com/#91251A934
Screw	91251A260	https://www.mcmaster.com/#91251A260
Washer	90107A011	https://www.mcmaster.com/#90107a011/=16t8lvh
Hex Standoff	91780A245	https://www.mcmaster.com/#91780a245/=16tr1ap
Nut	91841A011	https://www.mcmaster.com/#91841a011/=16r0qtd
Steel drive tube	4830K116	https://www.mcmaster.com/#4830k116/=16pnfxf
Aluminum drive tube	44665K117	https://www.mcmaster.com/#44665k117/=16sqd9c
Brass hose barb	WP7362568	https://goo.gl/RISnV4
Guide rods (flexure stage)	8890K183	https://www.mcmaster.com/#8890k183/=17ev8ns
Set screws	92765A311	https://www.mcmaster.com/#92765a311/=17eu0v9
Guide pins (compression screw)	98381A554	https://www.mcmaster.com/#98381a554/=16trgpd
Knurled-Rim Knob	6079K33	https://www.mcmaster.com/#6079k33/=16sq0j8
Compression Spring	9657K399	https://www.mcmaster.com/#9657k399/=16q6l6o
Steal bar stock	9517K433	https://www1.mcmaster.com/#9517k433/=17eu8b6
Ni-Cr wire	8880K11	https://www.mcmaster.com/#8880k11/=17euypv
Round Seal	12975K35	https://www.mcmaster.com/#12975k35/=16twv9t
Plastic tubing	51135K16	https://www.mcmaster.com/#51135k16/=17eu5vw

References

[1] **Christian Lomascolo, Mohit Maddipati, Nirmal Hari, Sarath David John, Wenjun Kang**, *"Thermally Actuated Flexure"*, Precision Machine Design, UNC Charlotte, 2015

[2] **J. Sam Jebar Kumar, Enoch Amoatey Tetteh, E. Paul Braineard**, *"A Study of Why Electrostatic Actuation Is Preferred and A Simulation of An Electrostatically Actuated Cantilever Beam for MEMS Applications"*, International Journal of Engineering Sciences & Emerging Technologies, Apr. 2014. ISSN: 22316604 Volume 6, Issue 5, pp: 441-446 ©IJESET

[3] **Daniel Amariei, Yvan Meason, Ion Vela,** *"Analysis and Design of Thermal Actuators"*, ANALELE Universitalii "EFTIMIE MURGU" Resila ANUL XIV, NR. 1, 2007, ISSN 1453 – 7397

[4] https://forums.ni.com/t5/Academic-Hardware-Products-ELVIS/myrio-vs-arduino/td-p/3270468. Date accessed: 8th April, 2017